ANALYSIS OF GENE SIGNATURES OF MIGRATORY PHENOTYPES USING THREE-DIMENSIONAL BREAST MICROTUMOR MODELS

by

Urmi Bharat Chheda

Bachelor of Technology, Institute of Chemical Technology, 2017.

Submitted to the Graduate Faculty of

School of Pharmacy in partial fulfillment

of the requirements for the degree of

Master of Science

University of Pittsburgh

2019

UNIVERSITY OF PITTSBURGH

SCHOOL OF PHARMACY

This thesis was presented

by

Urmi Bharat Chheda

It was defended on

April 4, 2019

and approved by

Dr. Shilpa Sant, Assistant Professor, School of Pharmacy

Dr. Da Yang, Assistant Professor, School of Pharmacy

Dr. Barry Gold, Professor, School of Pharmacy

Thesis Director Advisor: Dr. Shilpa Sant, Assistant Professor, School of Pharmacy

Copyright © by Urmi Bharat Chheda

2019

ANALYSIS OF GENE SIGNATURES OF MIGRATORY PHENOTYPES USING THREE-DIMENSIONAL BREAST MICROTUMOR MODELS

Urmi Bharat Chheda, B. Tech

University of Pittsburgh, 2019

Breast cancer is the second most common cause of cancer death in women. Yet, many challenges remain to be addressed such as treatment of local recurrence and metastasis; ability to predict the patients at risk of progression from pre-invasive to invasive disease; and overtreatment of patients that are not at risk. Recent studies show that the tumor microenvironment promotes acquisition of migratory phenotype by the tumor cells, which is one of the essential steps for pre-invasive to invasive transition. However, lack of experimental models with controlled tumor microenvironments to capture this transition is impeding progress in the field. To overcome the limitations of the current *in vitro* models, our lab has previously developed uniform-sized, three-dimensional (3D) *in vitro* microtumor models with controlled microenvironments using polyethylene glycol dimethacrylate (PEGDMA) hydrogel microwells. Without any external stimulus, the precise control over the size of T47D microtumors exhibits three key hallmarks of pre-invasive to invasive disease transition observed *in vivo*: increasing tumor size drives hypoxia and metabolic stress; heterogeneous tumor cells spontaneously emerge; and cells begin to migrate from the parent tumor. Thus, our lab has previously developed three controlled model systems: 1) non-hypoxic, non-migratory small microtumors (150μm/Day 6); 2) hypoxic, migratory large microtumors (600μm/Day 6); and 3) non-hypoxic, yet migratory small microtumors treated with tumor-secreted factors (secretome) from the conditioned media (CM) of large microtumors (150/CM Day 6).

The objective of this thesis was to analyze the gene signatures of migratory phenotypes using microarray data generated on these controlled breast microtumors (T47D). More specifically, the major goal was to delineate the role of hypoxic microenvironment, time of progression and tumor-secreted factors (CM) in inducing migratory phenotypes in non-migratory parental T47D cells. To understand the mechanisms of spontaneous emergence of migratory phenotypes in large hypoxic migratory microtumors (600μm/Day 6) and small non-hypoxic yet migratory microtumors (150/CM Day 6), we performed quantitative analysis of RNA expression using Affymetrix gene chip cDNA microarrays. We utilized non-hypoxic small microtumors (150μm/Day 6) and early stage large microtumors (600μm/Day 1) as controls of non-migratory phenotypes. The raw data were analyzed using Transcriptome Analysis Console (TAC) and Ingenuity Pathway Analysis (IPA). Our preliminary analyses show different genes affected by hypoxia in 600μm/Day 6 microtumors when compared to 600μm/Day 1 or 150μm/Day 6 tumors while no hypoxia-regulated genes were seen in 150/CM Day 6 microtumors when compared with 150μm/Day 6 microtumors. We discovered different sets of genes affecting migration function in large hypoxic microtumors (600μm/Day 6) and small CM-treated non-hypoxic microtumors (150/CM Day 6). Interestingly, experimental observations from our lab have revealed differences in the migratory pattern of these two microtumor models. Specifically, large hypoxic microtumors exhibited directional migration while CM-treated non-hypoxic small microtumors exhibited non-directional migration. Further studies are required to correlate the differences in the gene signatures identified by microarray analysis with the differences in these migration patterns. Thus, our controlled microtumors models may provide insights into different possible mechanisms implicated in the transition from non-migratory to migratory phenotypes. Future studies are underway to identify specific tumor secreted factors as potential biomarkers or therapeutic targets to halt primary tumor progression.

Table of Contents

Preface 1

1 INTRODUCTION 2

1.1 Pathophysiology of breast cancer 2

1.2 Current challenges in DCIS and IDC patients 3

1.3 DCIS to IDC transition 4

1.3.1 Tumor microenvironment (TME) 5

1.4 Cell culture models recapitulating DCIS microenvironments 6

1.5 In-house 3-D *in vitro* microtumor models with controlled tumor microenvironments 8

1.6 Gene expression profiling to identify markers for breast cancer progression 10

1.6.1 Studies using patient samples: A clinical perspective 13

1.6.2 Studies with *in vitro* 2-D and 3-D tumor models 15

1.7 Focus of Thesis 16

2 OVERVIEW OF THE MICROARRAY ANALYSIS PERFORMED 18

2.1 Transcriptome Analysis Console (TAC) 18

2.2 Ingenuity Pathway Analysis 19

2.2.1 IPA Knowledgebase 20

2.3 Clustering gene expression profiles of experimental groups 21

2.4 Statistical analysis of gene expression data 22

2.4.1 Intersection of genes in the analysis groups 23

2.5 Expression core analysis in IPA 23

2.5.1 Overlapping *p*-value 23

2.5.2 Z-score 24

2.6 Generating network of genes affecting migration function 24

2.6.1 List of genes affecting 'migration of cells' function from IPA Knowledgebase 24

2.6.2 Core analysis on the common genes 25

2.6.3 Selecting all networks with 'Cell Movement' as one of the Top Disease and Function 25

2.6.4 Building and overlaying 25

3 RESULTS AND DISCUSSION 26

3.1 Tumor Models 26

3.2 Hierarchical clustering of gene expression profiles 27

3.3 Temporal effect on pathways and biological functions of migratory phenotype 29

3.4 Effect of microtumor size (hypoxia) on pathways and biological functions 38

3.5 Effect of secretome (conditioned media of large microtumors, 600/CM) on migration of once non-migratory group 47

3.6 Comparison of the migratory signature between secretome-induced migration (150/CM Day 6) and hypoxia-induced migration (600μm/Day 6) 53

4 CONCLUSIONS AND FUTURE DIRECTIONS 60

5 ABBREVIATIONS 65

BIBLIOGRAPHY 70

List of Tables

Table 1: Analysis groups representing temporal, size or secretome effect on microtumor migration 26

Table 2: Genes common between 600µm/Day 6 *vs*. 600µm/Day 1 and genes resultant of hypoxic condition obtained from IPA knowledgebase 32

Table 3: Genes common between 600µm/Day 6 *vs*. 150µm/Day 6 and genes resultant of hypoxic condition obtained from IPA knowledgebase 40

List of Figures

Figure 1: Breast anatomy 2

Figure 2: Stages of breast cancer progression as per Wellings model 3

Figure 3: Photomicrographs of 150µm, 600µm and 150/CM microtumors at day 1 and 6 10

Figure 4: Steps involved in microarray experiment 12

Figure 5: Clariom_S_Human array's algorithm setting 19

Figure 6: Flow chart of analysis performed on microarray data used in the thesis 21

Figure 7: Overlap between genes of IPA knowledgebase and dataset 23

Figure 8: Hierarchical clustering of gene expression profiles of 150µm/Day 6, 600µm/Day 1, 600µm/Day 6 and 150/CM Day 6. 28

Figure 9: Analysis to identify top pathways affected by the microtumor size using migratory 600µm/Day 6 *vs.* non-migratory 600µm/Day 1 31

Figure 10: Relation between Hypoxia function and genes affecting hypoxia in 600µm/Day 6 *vs.* 600µm/Day 1 dataset 32

Figure 11: Directional effect of upstream regulators *BRD4* and *RARB* on migration functions via dataset genes 600µm/Day 6 *vs*. 600µm/Day 1 34

Figure 12: Network of extracellular molecules from the 600µm/Day 6 *vs.* 600µm/Day 1 dataset and the 'migration of cells' function including the canonical pathways through which the interaction between genes and function occurs. 36

Figure 13: Analysis to identify top pathways affected by the microtumor size using migratory 600µm/Day 6 *vs.* non-migratory 150µm/Day 6 39

Figure 14: Relation between Hypoxia function and genes affecting hypoxia in 600µm/Day 6 *vs.* 150µm/Day 6 dataset 41

Figure 15: Directional effect of upstream regulators *COL18A1* and *ER* on migration functions via dataset genes 600µm/Day 6 *vs.* 150µm/Day 6..... 43

Figure 16: Network of extracellular molecules from the 600µm/Day 6 *vs.* 150µm/Day 6 dataset and the 'migration of cells' function including the canonical pathways through which the interaction between genes and function occurs 45

Figure 17: Analysis to identify top pathways affected by the secretome using migratory 150/CM Day 6 *vs.* non-migratory150µm/Day 6 49

Figure 18: Network of extracellular molecules from the 150/CM Day 6 *vs.* 150µm/Day 6 dataset and the 'migration of cells' function including the canonical pathways through which the interaction between genes and function occurs 51

Figure 19: Different migratory pattern of A) 150/CM and B) 600µm microtumors on Day 6[75].. 53

Figure 20: Boxplot of Log-2 transformed mean expression values of 600µm/Day 6 and 150/CM Day 6..... 54

Figure 21: Pictorial representation of method used to obtain genes uncommon between 600µm/Day 6 and 150/CM Day 6 groups and affecting migration function..... 55

Figure 22: Network of genes from the 150/CM Day 6 group and the 'migration of cells' function including the canonical pathways through which the interaction between genes and function occurs 57

Figure 23: Network of genes from the 600µm/Day 6 group and the 'migration of cells' function including the canonical pathways through which the interaction between genes and function occurs 58

Preface

I would like to acknowledge the School of Pharmacy, University of Pittsburgh for granting me the opportunity to pursue my graduate studies. I express sincere gratitude to my advisor, Dr. Shilpa Sant for guidance, constant support and patience throughout my studies. I would like to thank Dr. Vinayak Sant for his valuable feedback and encouragement. I am thankful to Dr. Maggie Folan and other faculty from School of Pharmacy for their guidance. I would like to acknowledge Dr. Manjulata Singh for the training in technical skills, and mentorship during my studies. I express gratitude to Dr. Ansuman Chattopadhyay for his assistance with Ingenuity pathway analysis software. I would like to thank all past and current members of Sant Lab – Dr. Yingfei Xue, Akhil Patel, Nayyar Ahmed, Mrunal Sakharkar, Vishal Rakshe, and alumni for their unflinching assistance, feedback and support throughout my studies. Special thanks to Nayyar Ahmed for reviewing my thesis document. I would like to thank members from Dr. Da Yang's lab for their generous help with basics of gene analysis. I am thankful to Lori Altenbaugh for her kind help in administrative support. Finally, I express deep gratitude to my parents, grandparents, my brother Paras and friends whose constant support and care was essential in completion of my studies.

1 INTRODUCTION

1.1 Pathophysiology of breast cancer

Breast cancer, which stands for uncontrolled growth of breast cells[1-2] is the second most common cancer in women. The American Cancer Society has estimated 42,260 deaths in the year 2019 due to breast cancer, inclusive of both sexes[3].

Breasts or mammary glands are made up of lobules (responsible for milk production), and ducts (responsible of milk transport to nipple) as shown in **Figure 1**[4-5]. Breast cancer is a heterogeneous disease with ductal and lobular breast carcinomas as the most common types and ductal carcinoma accounting for 40-75% of all diagnosed cases[6].

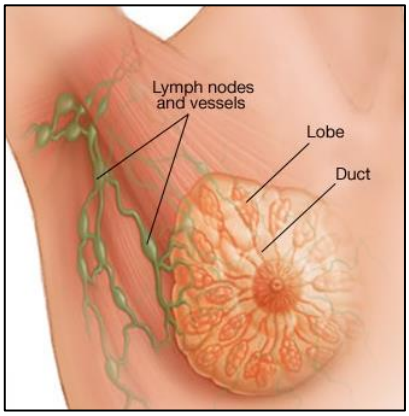

Figure 1: Breast anatomy[4]

For ductal carcinomas, there are two proposed models of progression, but the model proposed by Wellings and colleagues is considered valid after immuno-histochemical and biological evidence. This model proposes following stages of progression: pre-malignant stages, viz., ductal hyperplasia (DH), atypical ductal hyperplasia (ADH) and malignant stages, viz., ductal carcinoma

in situ (DCIS) and the invasive stage called invasive ductal carcinoma (IDC) as shown in **Figure 2**[7-6] . Invasive ductal carcinoma represents nearly 80% of breast cancer diagnoses[8].

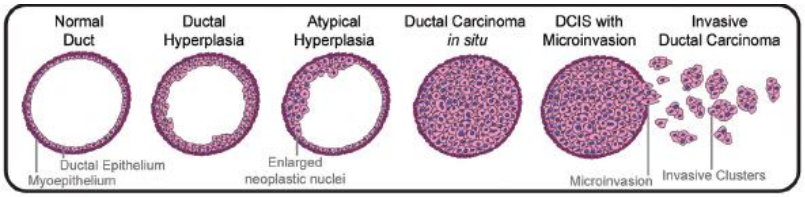

Figure 2: Stages of breast cancer progression as per Wellings model[7]

1.2 Current challenges in DCIS and IDC patients

Despite of the increasing research in the field of breast cancer, there are still major challenges to be addressed. These are, 1) recurrence or metastasis of tumor; 2) inability to predict disease progression from pre-invasive to invasive disease[9-10]; 3) overtreatment of patients that are not at risk of progression to invasive disease[7, 11-12]. Based on diagnosis of the cancer, the decision of lumpectomy plus radiation therapy or mastectomy might result into tumor recurrence and metastasis [13].

With the advent of mammography, early detection of non-palpable mass is made possible reducing the breast cancer mortality by 19%[14-15]. In case of techniques of pathological evaluation, it is challenging to distinguish between closely related diseases such as DCIS and DCIS with microinvasion. Accurate sizing of tumor tissue can also be challenging if there is presence of normal tissue within the tumor mass or change in the tumor size due to breast tissue elasticity. Presently, protein expression assays of HER2/NEU (or HER2, human epidermal growth factor receptor 2), ER (estrogen receptor) and PR (progesterone receptor) proteins are used in conjunction with current diagnostic approaches, but histological markers are limited due to intra- and inter-tumoral variations[16]. Therefore, advanced research on biomarkers for better breast cancer diagnosis and prognosis is required in addition to current clinical techniques. Similarly, identifying

the factors involved in the progression of early stage pre-invasive breast cancer to invasive stage is necessary to halt tumor progression at the pre-invasive stage. Such knowledge can also help prevent overtreatment of patients that are not at risk of invasive disease.

1.3 DCIS to IDC transition

Cell migration and invasion (cell movement through extracellular matrix (ECM) or infiltrating neighboring tissues) are the initial steps of tumor progression, which involves chemotactic movement of tumor cells, assisted by protrusive activity of cell membrane and attachment to the ECM[17]. Breast cancer cells first invade the basement membrane and then migrate out of the breast duct[18]. There are two models proposed for DCIS to IDC transition: the 'escape' and the 'release' model[19]. The 'escape' model proposes that the genetic changes in the epithelial cells enable them to invade the ducts. However, some recent studies have shown the genomic similarity between DCIS and IDC and significant differences between DCIS and normal epithelial cells[20-25]. Ma *et al.*[26] analyzed gene expression profiles of different stages of breast cancer progression within a patient and between patients on a cohort of 36 patients. Their findings show that many genetic abnormalities present in the DCIS and the IDC stages were pre-existent at the ADH stage. Hence, there may be other non-genomic factors leading to DCIS-IDC progression.

The 'release' model for DCIS-IDC transition proposes that the abnormal microenvironment drives the disruption of basal membrane and migration of cells[19]. There is a non-genetic theory that tumor microenvironment (TME) might be responsible for triggering DCIS-IDC transition.[27-28] Hence, TME has been studied widely to understand features of DCIS-IDC transition such as cell migration and invasion[29].

1.3.1 Tumor microenvironment (TME)

TME consists of non-cellular components such as availability of nutrients and oxygen, cellular components such as the tumor cells and non-tumor cells (*e. g.*, myoepithelial cells, fibroblasts, immune cells, etc.), tumor secretome (factors secreted by tumor and non-tumor cells in response to the evolving environment), and the ECM surrounding the tumor[30-32]. Non-cellular factors of tumor microenvironment, viz., hypoxia or reduced oxygen tension[24], and metabolic stress have been reported to promote metastases via tumor cell migration, and invasion.[33-36] Hypoxia represents inadequate intra-tumor oxygen delivery which leads to increased *HIF-1* (hypoxia-inducible factor 1) expression.[37] It is the key feature of tumor microenvironment that directs metastatic potential of the tumor cells.[33] Carmen Chak-Lui Wong *et al.* [38] reported that *HIF-1* is an important regulator of breast cancer progression. Similar to hypoxia, metabolic stress or nutrient deprivation is the hallmark of many malignancies.[39] Tumor response to metabolic stress to maintain cellular bioenergetics contributes to tumor progression and metastases.[40] It is well known that the tumor cells secrete certain factors called the tumor secretome to cope with the constantly changing environmental conditions[41]. The secreted factors belong to important class of molecules such as extracellular proteases, cell motility factors, growth factors, cytokines, chemokines, angiogenic factors, anti-survival proteins and other bioactive molecules. It is reported that matrix metalloproteases (MMPs) such as *MMP2* and *MMP14* expression is elevated during DCIS to IDC progression[42]. *TGFBR2*, *SMAD4*, or *GLI1* downregulation in MCF10DCIS.COM cells (human DCIS cell line) enhanced progression to invasive stage[43].

Apart from conditional factors like hypoxia, tumor cell-cell interactions and cell-ECM interactions also drive the emergence of heterogeneous tumor cell phenotypes[44]. The differences in survival, growth, invasive and metastatic ability of the heterogeneous phenotypes regulate cell migration,

invasion and metastasis[44] making emergence of heterogeneous phenotype as another hallmark of tumor progression.

1.4 Cell culture models recapitulating DCIS microenvironments

The cell-cell, and cell-ECM interactions, and tumor secretome are widely studied in two-dimensional (2-D) and three-dimensional (3-D) cultures. Porter *et al.*[45] reported the loss of *SIM2s* (single-minded) in 2-D monocultures of MCF10DCIS.COM cells (human DCIS cell line) when compared to the non-transformed parent MCF10A cells, but the expression was higher as compared to MCF7 and MDA-MB-231 cells. To study the oncogenic role of myoepithelial cells in DCIS-IDC transition, Pang-Kuo Lo *et al.*[23] co-cultured 2-D MCF10DCIS.COM and Hs578bst (tumor-associated myoepithelial cell line) cells in the same cell culture dish. Elevated expression of *FOXC2* (forkhead box protein C2), *SNAIL* (zinc finger protein SNAI1), *ZEB1* (zinc finger E-box binding homeobox 1), *ZEB2* (zinc finger E-box binding homeobox 2), and *Vimentin* and decreased expression of *E-cadherin* was observed in co-cultured MCF10DCIS.COM cells in comparison with monocultures. Kelly *et al.* [46] co-cultured SUM149 or SUM102 2-D breast cancer cell lines with RMF-HGF fibroblast cells to study the level of MET phosphorylation. Zhou *et al.*[47] observed breast cancer cells (MCF10DCIS.COM) migration by co-culturing them with PCS-500-011 (human adipose-derived MSCs) cells in 2-D cultures.

While 2-D cell culture is widely used for its ease and convenience, it is increasingly accepted that these monolayer cultures of cancer cells are too simplistic and do not recapitulate important aspects of *in vivo* microenvironments such as cell-cell interactions, cell-ECM interactions and nutrient availability[48]. In order to recapitulate *in vivo* environment, we need to consider 3-D context of TME. For example, as DCIS lesions grow beyond 150-200 μm, the tumor cells experience oxygen and nutrient gradients creating a hypoxic core due to lack of oxygen and nutrient supply[49]. Indeed,

presence of prevalent hypoxia is one of the hallmarks of DCIS[50]. Hence, there is an increasing interest in developing 3D tumor models in the cancer community to recapitulate some of the hallmarks of the *in vivo* TME[51]. Following are examples of studies that used 3-D culturing techniques to study effect of TME on DCIS-IDC transition.

Edward *et al.*[52] performed 3-D co-culture of myoepithelial and luminal cells obtained from ductal organoids in collagen gels to understand the cross-talk between the two cell types and effect on breast cancer progression. Kingsley *et al.*[53] co-cultured DCIS cells (MCF10DCIS.COM and SUM102) and stromal carcinoma-associated fibroblast cells (CAF40T) in 3-D, which were sandwiched between Cultrex (a basement membrane matrix). The authors concluded that *IL-6* (interleukin-6) signaling between the two cell types plays a crucial role in DCIS-IDC progression. Lauren *et al.*[54] demonstrated induction of invasion of DCIS by co-culturing HMFs (human mammary fibroblasts) with MCF10DCIS.COM cells in 3-D in triple microchannels with single channels connected by diffusion channels. Ying W. *et al*.[55] encapsulated 21PT and 21MT-2 breast cancer cell lines into hydrogels, which were maintained at hypoxic conditions. They showed that hypoxia increased cell migration along with expression of *LOX*.

Major limitation of many of the current 3-D models such as spheroid systems is their inconsistent tumor sizes, which may be the cause of non-reproducible results due to batch-to-batch variations *in vitro*.[56] Lack of high throughput methods, and inability to support long term cell growth are other shortcomings of existing 3-D tumor models. There are studies that use hypoxic chambers to generate hypoxia in 2-D cell monolayers or even spheroid cultures.[57-58] These studies are unable to reproduce the spatial oxygen gradients and spatial phenotypic heterogeneity observed *in vivo*, where only an inner hypoxic core exists. This is because, in hypoxic chambers, all cells in 2-D and even outer cells in 3-D spheroid cultures are exposed to hypoxia. Therefore, it is desirable to have

a high throughput 3-D experimental system that recapitulates a spontaneously formed hypoxic tumor microenvironment without interference from other non-cancerous cells.

1.5 In-house 3-D *in vitro* microtumor models with controlled tumor microenvironments

Currently, there are no preclinical *in vitro* models that show tumor progression in real time in the same tumor model using the same cell line without any genetic manipulations or any artificial culture conditions[30, 51, 59-61]. Our lab has previously engineered an array of uniform size hydrogel microwells using microfabricated polydimethylsiloxane (PDMS) microposts of defined diameter and height. The hydrogel microwells are made of polyethylene glycol dimethacrylate (PEGDMA), a non-adhesive polymer that does not allow cell-hydrogel interaction, and thus, maximizes cell-cell interaction[30, 51, 59-61] forming hundreds of uniform size cell aggregates (referred henceforth as 'microtumors'). The size of microtumor is determined by the diameter of the microwells on the array, the compaction ability of the cells used and the cell seeding density [30, 59]. For example, T47D breast cancer cells seeded on a device containing 150 μm diameter hydrogel microwells result in microtumors of average diameter of 128 ± 16 μm (referred as 'small' microtumors) while that containing 600 μm diameter hydrogel microwells result in microtumors of average diameter of 550 ± 57 μm (referred as 'large' microtumors) by day 6.[60] Each 1x1 cm^2 device of 150 μm size microwell generates 350-450 small microtumors while each 1x1 cm^2 device of 600 μm size microwell generates 60-70 large microtumors.[30] The tumors are allowed to grow for 6 days after which they are harvested and stored for further analysis. Previous studies from our lab have shown that large T47D microtumors develop hypoxic areas unlike small microtumors.[30, 60, 62] Our lab has also shown that without any additional stimulus, large T47D microtumors exhibit migratory phenotype as early as day 3-4 while small T47D microtumors generated from the same parent cells

never migrate as seen in **Figure 3**[59, 30, 60] In addition, our previous studies have also shown emergence of heterogeneous cellular population based on the expression of epithelial marker, E-Cadherin (E-CAD) and mesenchymal marker, Vimentin (VIM).[59] In conclusion, the hydrogel microwell platform can generate hundreds of defined yet uniform size microtumors from the same parent cells. Without any external stimulus, and artificial culture conditions such as hypoxic chambers and genetic manipulations, the precise control over the microtumor size leads to controlled hypoxic and metabolic tumor microenvironments. Importantly, these microtumor models recapitulate three key hallmarks of pre-invasive to invasive disease progression that is observed *in vivo*: 1) Increasing tumor size drives hypoxia and metabolic stress; 2) Heterogeneous tumor cells spontaneously emerge; and 3) Cells begin to migrate from the parent tumor. Thus, these large hypoxic and migratory large microtumors allow us to study effect of time of progression (comparison between 600μm/Day 1 to 600μm/Day 6) and hypoxic microenvironments (comparison between 600μm/ Day 6 to 150μm/ Day 6).

Our lab has also studied the effect of tumor secreted factors in inducing microtumor migration in otherwise non-migratory small (150μm) microtumors and have shown that when treated with 50% conditioned media of large microtumors starting from day 3, these non-migratory small microtumors started migrating (**Figure 3C**)[59]. Interestingly, these experiments revealed differences in migration pattern between hypoxic 600μm/ Day 6 and 150CM/Day 6. Specifically, large hypoxic microtumors exhibited directional migration while CM-treated non-hypoxic small microtumors exhibited non-directional migration. Hence, this model would give us better understanding of secretome specific effect on migration of once non-migratory small non-hypoxic microtumors.

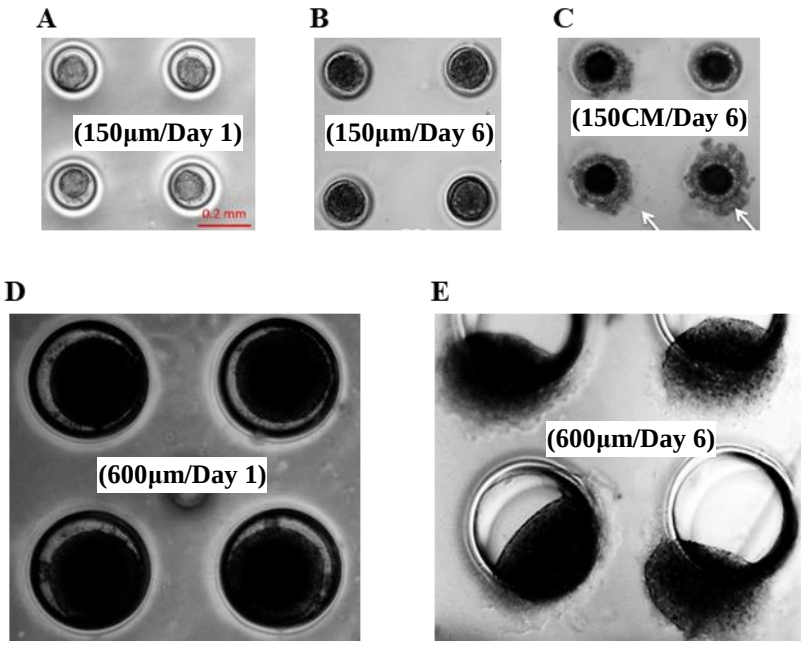

Figure 3: Photomicrographs of 150µm, 600µm and 150/CM microtumors at day 1 and 6[59]

All images were taken at 4X magnification.

A) Untreated 150µm microtumors on day 1 (150µm/Day 1); **B)** Untreated 150µm microtumors on day 6 (150µm/Day 6); **C)** 150µm microtumors treated with conditioned media of 600µm microtumor from day 3-6(150CM/Day 6) **D)** 600µm tumor on day 1 (600µm/Day 1); **E)** 600µm tumor on day 6 (600µm/Day 6)

Further molecular understanding is essential to reason out the possible transition from non-migratory to migratory phenotype in our *in vitro* 3-D tumor models.

1.6 Gene expression profiling to identify markers for breast cancer progression

It was thought that the gene expression profile of tumors in the late stage of a known cancer phenotype can be used to develop a gene database that would in turn give better knowledge about

progression of unknown phenotypes. To support this hypothesis, there are many studies focused on genes affecting breast cancer progression, migration and invasion. Some studies used validation approaches to test the expression of a single gene or small array of genes on tumor progression, migration and/or invasion. For instance, Xu *et al.*[63] demonstrated role of *TWIST1* in inducing migration and invasion by silencing *FOXA1* expression in breast tumors. *CCL2/CCR2* overexpression has been reported to be associated with metastatic breast cancer.[64] Lin *et al.*[65] showed the positive effect of *CCR10* activation on breast cancer migration and invasion via ERK1/2/MMP-7 signaling pathway. Other studies have used whole genome expression analysis to obtain expression profiles of a large array of genes affecting progression and migration of breast cancer.

One of the two techniques commonly used to quantify large array of transcribed genes are microarrays and RNA sequencing (RNA-seq). Analyzing gene expression profiles of large array of genes can help us develop a better understanding about the biological state and genes expressed in that stage. Both the techniques work on cDNA reverse transcribed from mRNA extracted from cells, but, in case of RNA-seq, mRNA is selectively filtered using poly (A) selection, which is done by mixing RNA with poly (T) oligomers. For RNA-seq technique, cDNA is fragmented and sizes within a tight range are selected. Adapters are attached on both ends of cDNA fragments and with or without amplification, each molecule is sequenced. The results are aligned to reference genome or they are *de novo.*[66] In case of microarrays, two-channel or single-channel technologies are used as shown in Figure 4[67]. In microarray experiments, probe is the nucleotide sequence attached to the microarray surface while target is the sequence hybridized to the probe.[67]

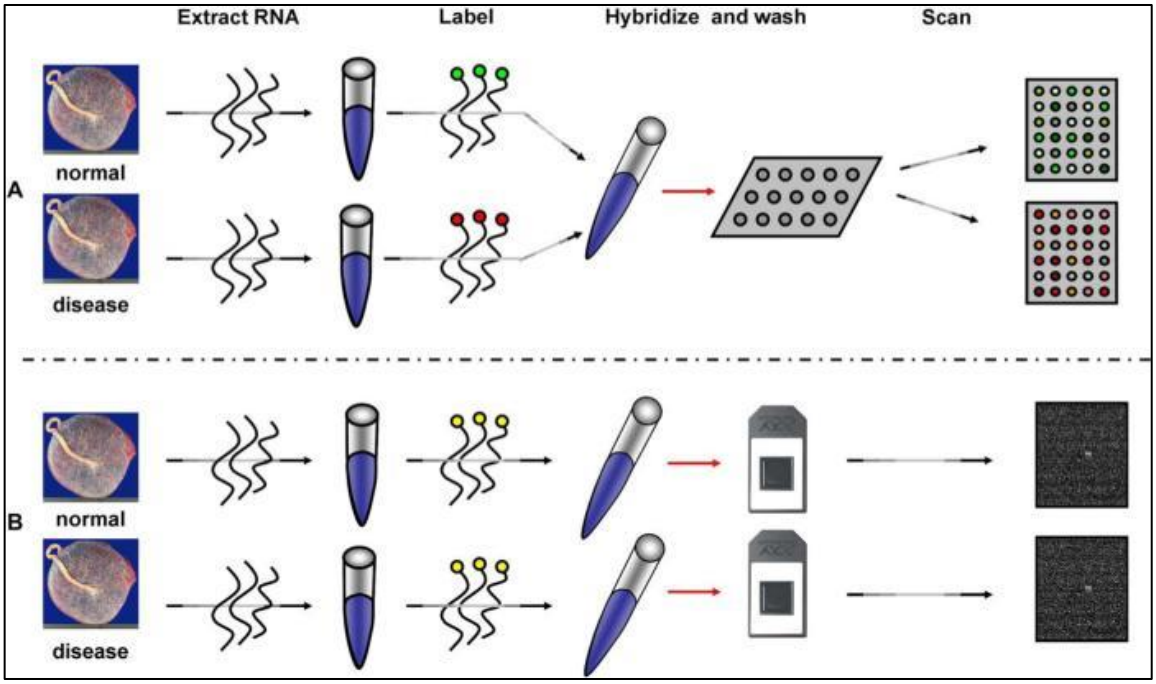

Figure 4: Steps involved in microarray experiment[67]

A) Two-channel Technology, B) Single-channel Technology

A) Two-channel technology involves RNA extraction from two different samples, which are labeled with two different fluorescent dyes before mixing and are then hybridized on the same microarray. B) In single-channel technology, RNAs from two separate samples are not mixed and are labeled with the same dye and hybridized on different arrays. The arrays are then washed and scanned at different (A) or same (B) wavelength.

Analysis done on microarray data using bioinformatics tools is vastly used for deriving hypotheses for future aims. Microarrays can be used to either compare two sets of gene expression profiles or to match the gene profile of a test sample with that of the control or to obtain a gene expression profile of a standard with which other samples can be compared. Nazarov *et al.*[68] compared Affymetrix HTA 2.0 microarray with Illumina 2000 RNA-seq for the analysis of lung carcinomas. Stochastic variability was found to be higher in case of RNA-seq than microarray. This variability resulted in the lack of reads for short and low-abundant genes such as lncRNAs (long non-coding RNAs). Despite that, gene expression analysis results were consistent between the two techniques.

Both techniques have their advantages and drawbacks. For performing gene expression analysis of a genome with reference sequence, microarray is the preferred technology while for discovery of novel transcripts and allele-specific expression and identification of alternatively spliced genes, RNA-seq is the preferred technology.[69] RNA-seq is most useful when the genomic sequence is unknown whereas in case of microarrays, prior knowledge of nucleic acids is required.[70]

RNA-seq is more sensitive than microarray identifying more genes than microarray. Also, many studies found RNA-seq to be more accurate than microarray in terms of fold change values.[71] While RNA-seq has many advantages over microarrays, scientists still prefer microarray technologies due to their lower cost, availability of a standard protocol, lower file size (less than one gigabyte for microarray and greater than two gigabytes in compressed format for RNA-seq files), and easier analysis tools.[72] Despite of the size of data of RNA-seq, the processed count data for each gene is equivalent to processed microarray intensities. Large data files of RNA-seq makes data storage and sharing difficult.[73]

To study the markers of breast cancer progression, patient samples, 2-D or 3-D breast tumor models using primary cells or cell lines have been used. Some of these studies along with their shortcomings have been discussed below.

1.6.1 Studies using patient samples: A clinical perspective

Ma *et al.*[26] analyzed gene expression profile in different stages of breast cancer patients and showed high levels of expression of *CKS2, RRM2,* and *UBE2C* genes in IDC compared to DCIS. Sgroi DC *et al.*[74] combined laser capture microdissection (LCM), a technique used for procurement of cells from specific microscopic regions of tissue samples, and cDNA (complementary DNA) microarrays to study expression profile of more than 8000 genes from normal epithelial cells, malignant invasive cells and malignant metastatic cells derived from the same patient. After

validating with RT-qPCR (real-time quantitative polymerase chain reaction), *APOD, BRCA1, CCL5* genes were found to be upregulated in invasive carcinoma cells and *ARBK1, HSF1, ANXA1* genes were upregulated in metastatic carcinoma cells while *APOD* gene was downregulated in metastatic carcinoma cells. Similar cell procurement technique was used by Luzzi *et al.*[75] to obtain patient-matched pre-malignant and malignant cells from breast cancer samples. They found that LF protein was upregulated in patients 1 and 2 but downregulated in patient 3 when compared to non-malignant epithelium. *PS2* and *SIX1* were upregulated and *SPARCL1* and *OXTR* were downregulated in DCIS *vs*. normal epithelium in patient 1 and 3 while reverse was observed in patient 1. Some studies use non-human xenograft models to study breast cancer progression but tissue composition, nutrient type, and mechanisms affecting cancer growth, survival and progression in animal xenografts may differ from human disease[76].

Even though patient samples have used for biomarker discovery, there are certain shortcomings of working with patient derived tissues. One such drawback is the storage of tissue sample[77]. Tissue samples are either stored for further analysis by fixed formalin paraffin (FFPE) embedded method or freezing the samples. Both methods affect the tissue samples critically, thus they may influence future analysis and results. Frozen samples are prone to rapid deterioration once exposed to room temperature. Apart from tissue quality, purity of cell population is not guaranteed in patient samples.[78] Also, availability of matched patient pairs and specific cohorts is difficult, which might lead to small sample sizes. Due to high inter-patient variations, large sample size is generally required to produce clinically significant results.

To overcome these challenges related to the patient samples, *in vitro* tumor models are often used in the quest of identifying reliable biomarkers for breast cancer progression.

1.6.2 Studies with *in vitro* 2-D and 3-D tumor models

Geiger *et al.*[79] used mass spectroscopy (MS) to carry out deep analyses of proteomes from 2-D cell cultures of cells obtained from tumors at defined breast cancer stages. They used cells at pre-malignant (MCF10a and HMT-3522-S1 cells), stage II (HCC1143 and HCC1937 cells), stage III (HCC202, HCC2218, and HCC1599 cells), and metastatic cells from pleural effusions (MFM223 and MDA-MB-453 cells). The results obtained using cell lines were validated using breast cancer tissue arrays. The authors found that *IDH2* and *CRABP2* levels increased while *ANX3* levels decreased with tumor stage. Calaf *et al.*[80] studied the expression of c-Ha-Ras protein (responsible for control of cell growth) in 2-D breast cancer cells of normal breast epithelial cells (MCF-10F), malignant and tumorigenic cell line (Alpha5 cells) and in biopsies of normal, benign and malignant breast tumors from different patients using immunohistochemistry. Malignant cell line and malignant breast tumor biopsies showed positive expression of c-Ha-Ras protein while normal epithelial cells were negative for c-Ha-Ras expression. Lin *et al.*[65] used 2-D breast cancer cell lines to show the positive effect of *CCR10* activation on breast cancer migration and invasion via ERK1/2/MMP-7 signaling pathway. Sarah *et al.*[81] performed RNA-seq on RNA extracted from 3-D spheroids of isogenic MCF10 progression series (MCF10DCIS.COM, MCF10Ca1a, MCF10Ca1d, and MCF10Ca1h cells). They reported increased expression of *TPRD*, *TP53*, and *VSP13A* genes in MCF10Ca1a and MCF10Ca1h cells when compared to MCF10DCIS.COM.

Due to the drawbacks of 2-D cultures and current 3-D breast tumor models discussed in section 1.4, the use of the *in vitro 3-D* model discussed in section 1.5 will help us study the molecular changes driving the DCIS to IDC progression.

As mentioned earlier and in previous publications from the lab[30, 60], the microtumor models were fabricated from T47D breast cancer cell line, which represents luminal A (ER+/PR+/HER2-)

molecular subtype of breast cancer. T47D cells are epithelial cells derived from pleural effusion of a 54-year-old female with invasive ductal carcinoma or IDC. The advantage of these controlled microtumor models is that it enables controlled comparisons between non-migratory (150µm/Day 6 and 600 µm/Day 1) and migratory groups (600µm/Day 6 and 150CM/Day 6) to understand the gene expression changes occurring due to the hypoxia (created by engineering microtumor size), time of culture and secretome.

In this thesis, we performed microarray data analysis by leveraging this already developed 3D T47D microtumor models with controlled microenvironments as listed below.

1) Small (150µm) microtumors harvested on day six (**Figure 3B**, 150µm/Day 6, non-hypoxic, non-migratory)

2) Large (600µm) microtumors harvested on day one (**Figure 3D**, 600µm/Day 1, non-migratory)

3) Large (600µm) microtumors harvested on day six (**Figure 3E**, 600µm/Day 6, hypoxic, migratory)

4) Small (150µm) microtumors harvested on day six after treatment with conditioned media of large microtumors starting from day 3 (**Figure 3C**, 150/CM Day 6, non-hypoxic, yet migratory).

The microarray experiment was performed using single channel technology of Affymetrix Clariom S assay for Humans.

1.7 Focus of Thesis

The major objective of this thesis was to analyze the gene signatures of migratory phenotypes using microarray data generated on these controlled breast microtumors (T47D). More specifically, the major goal was to delineate the role of hypoxic microenvironment, time of progression and tumor-secreted factors (CM) in inducing migratory phenotypes in non-migratory parental T47D cells. This was accomplished in following specific aims:

AIM 1: To investigate effect of hypoxic microenvironments, time of progression and secretome on the emergence of migratory phenotype in otherwise non-migratory microtumors fabricated from the same parent cells

AIM 2: To investigate unique genes responsible for the difference in the migratory behavior between large hypoxic migratory microtumors (600μm/ Day 6) and small non-hypoxic yet migratory tumors (150CM/ Day 6).

2 OVERVIEW OF THE MICROARRAY ANALYSIS PERFORMED

Transcriptome analysis console (TAC) 4.0 and Ingenuity Pathway Analysis (IPA) were used to analyze the results generated from the experiments.

2.1 Transcriptome Analysis Console (TAC)

TAC 4.0 has combined features of Expression Console 1.4 and TAC 3.1. Expression console performs gene level normalization and signal summarization to give .CHP files (contains gene expression values) on which TAC 3.1 performs statistical analysis.

Firstly, the required library files were downloaded in a specific folder on the local computer. Library files downloaded were Clariom_S_Human. TAC 4.0 utilizes limma, which is a part of Bioconductor software package and ANOVA method selected for gene expression analysis was eBayes (default). Figure 5 shows the Clariom_S_Human array's algorithm setting.

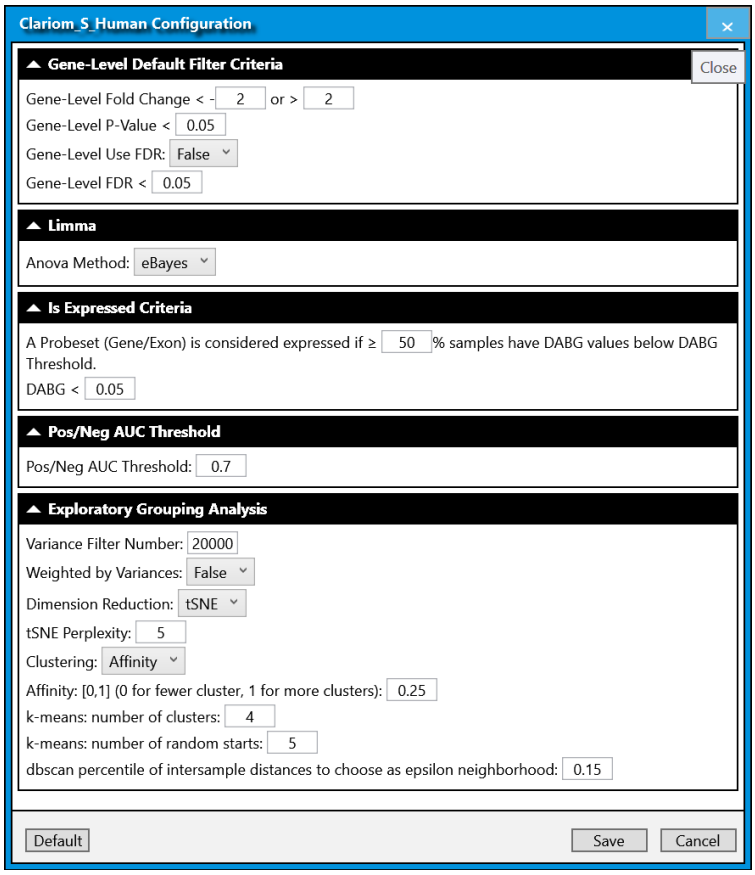

Figure 5: Clariom_S_Human array's algorithm setting

2.2 Ingenuity Pathway Analysis

Ingenuity Pathway Analysis or IPA is a user-friendly web-based software application for interpretation of data from -omics experiments such as microarrays. Apart from pathway enrichment analysis, IPA can identify key upstream regulators, and downstream effects from a dataset. Interactive networks between genes and function can also be built along with predicted activation or inhibition of the function/disease, a feature present only in IPA amongst other bioinformatics software. IPA allows targeted analysis specific to a gene or function of disease. This facilitates biomarker identification and discovery of a therapeutic target.

There are four causal analytics algorithms in IPA: 1) Upstream regulator analysis (URA) 2) Mechanistic networks (MN) 3) Causal Network analysis (CNA), and 4) Downstream effect analysis (DEA).

2.2.1 IPA Knowledgebase

Ingenuity pathway knowledgebase is a collection of observations from various experiments manually curated to obtain nearly 5 million findings from literature of top journals or third-party databases. It contains nearly 40,000 nodes representing mammalian genes, gene products, microRNA, chemical compounds and biological functions, which are connected by nearly 1,480,000 edges. The edges represent the causal effect and its direction, viz. activation or inhibition.[82]

Figure 6 represents the flow chart for the analysis performed further in the thesis.

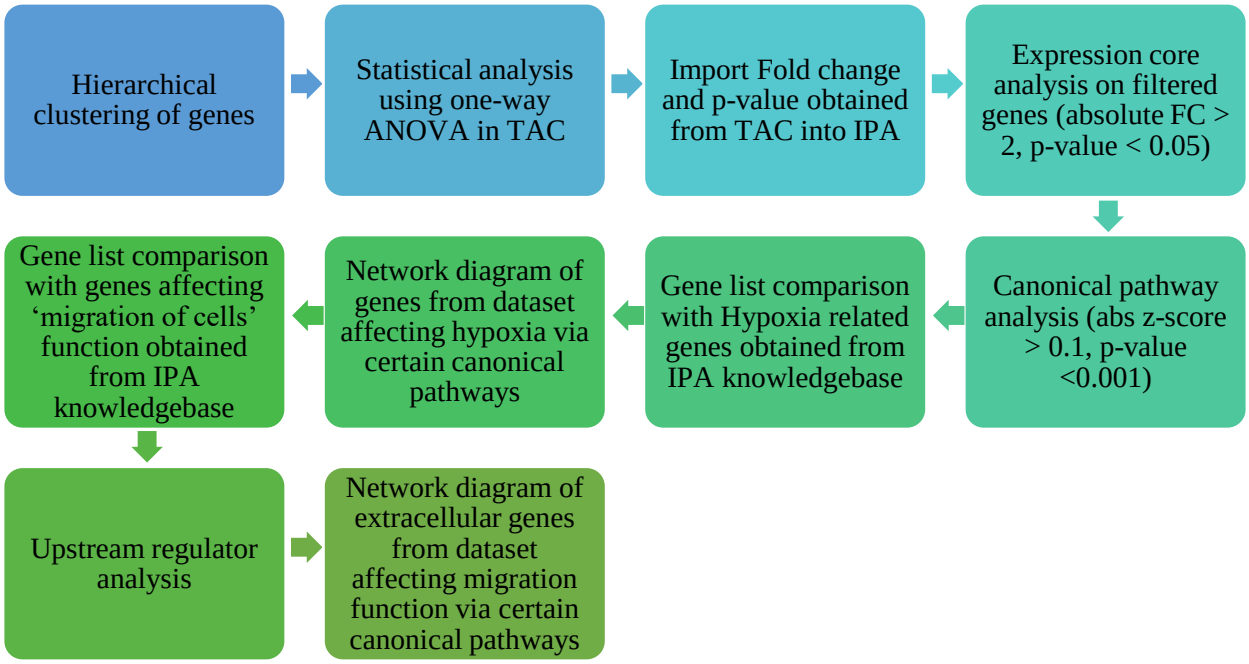

Figure 6: Flow chart of analysis performed on microarray data used in the thesis

2.3 Clustering gene expression profiles of experimental groups

Raw gene expression data from Affymetrix GeneChip Scanner (.CEL) of all experimental group replicates were imported into Transcriptome Analysis Console (TAC) and sample attributes (names assigned to each .CEL (contains probe-level intensities) file imported) were directly added. TAC considers files with same sample attribute as replicates of a sample.

Hierarchical clustering was performed in TAC, where samples with similar gene expression profiles are grouped together. To build this hierarchical tree, only those genes, which have expression values in all samples, are considered. Hierarchical clustering type used here is agglomerative clustering which has a bottom-up approach. Initially, each object is considered as a single-cluster and at each step of algorithm, two clusters that are most similar are combined under one cluster. This continues until all the objects are under one big cluster. Complete-linkage

clustering method is used to obtain distance between clusters of samples. The distance between two clusters is defined by the longest distance between two points in those clusters. Results were presented as a heat map and dendrogram. Log2-transformed expression values were plotted in the heat map.

2.4 Statistical analysis of gene expression data

Two experimental groups (considered as 2 conditions in TAC) were imported for analysis at a time, viz. triplicates of 600µm/Day 6 group and of 600µm/Day 1 group were imported together and statistical analyses was performed using one-way ANOVA to test the effect of time on microtumor migration. Analysis summary showed the number of genes differentially expressed between the two groups (number of genes upregulated or downregulated). TAC 4.0 presents a gene table with Tukey bi-weight average of the expression values for each ID of all replicates of a condition, Fold-change (condition 1 *vs.* condition 2), *p*-value and FDR (false discovery rate) *p*-value.

Fold Change (FC) of condition 1 *vs*. condition 2:
If $\log_2$(condition 1) > $\log_2$(condition 2), then:

$$FC = 2^{(log_2(condition\ 1) - log_2(condition\ 2))}$$

Otherwise,

$$Fold\ change\ (FC) = -2^{(log_2(condition\ 1) - log_2(condition\ 2))}$$

To identify the molecular signature of the migratory phenotype, we compared differential gene expression between migratory (e.g. 600µm/Day6, condition 1) *vs.* non-migratory (e.g. 600µm/Day1, condition 2) group. The genes with absolute fold change (FC) values greater than 2 and *p*-value less than 0.05 were used for further pathway and functional analysis in IPA.

2.4.1 Intersection of genes in the analysis groups

TAC generates Venn diagrams representing differential gene expression. It gives the number of common and uncommon genes between two or more datasets. By selecting the list of common or uncommon genes in a comparison, TAC generated the list, which was exported for future analysis.

2.5 Expression core analysis in IPA

Expression core analysis was performed on filtered gene set for each analysis obtained from the TAC along with their *p*-value and fold change. The fold change in gene expression between the two groups was used to evaluate the directionality (z-score) of analysis. No cutoffs were set; analysis was performed on the entire dataset.

Canonical pathways with particular *p*-value and absolute z-score were filtered resulting in top pathways that are significantly activated or inhibited.

2.5.1 Overlapping *p*-value

Overlapping *p*-value is calculated using right tailed Fisher's exact test different from expression *p*-value of dataset. Direction of gene expression is not considered in this calculation. The statistical test was used to find the overlap between the dataset genes and genes in the IPA knowledgebase

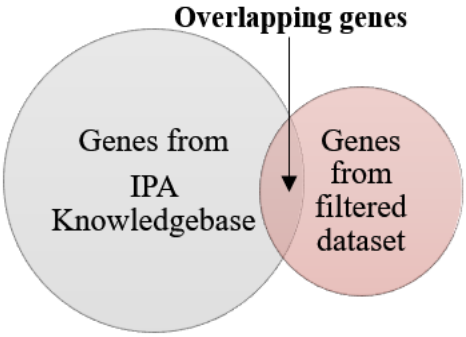

Figure 7: Overlap between genes of IPA knowledgebase and dataset

as shown in **Figure 7**. In case of canonical pathways, the genes in the canonical pathways and the dataset genes are overlapped.

2.5.2 Z-score

Z-score is the statistical measure of the match between observed gene expression and expected gene relationship direction. Formula for z-score is as follows:

$z - score = \frac{N(+) - N(-)}{\sqrt{N}}$ where, N (+) is the number of genes, where the observed gene expression is consistent with the expected direction while N (-) is the number of genes, where the observed gene expression is consistent with the expected direction.

2.6 Generating network of genes affecting migration function

Since there are 4510 molecules in IPA Knowledgebase that affect migration function, *p*-value of the function for an analysis group might not be significant due to relatively smaller number of genes responsible for migration present in the analysis group dataset. Hence, to obtain more specific interaction network between dataset genes and migration function, genes specific to migration function were filtered from our analysis group datasets by carrying out the following steps.

2.6.1 List of genes affecting 'migration of cells' function from IPA Knowledgebase

List of genes affecting 'migration of cells' function was obtained from IPA knowledgebase and a new list was created with this data. This list was then compared to gene list of an analysis group to obtain list of common genes labeled as "*analysisgroup_common_migrationofcells".*

2.6.2 Core analysis on the common genes

Since the 'compare' function simply generated the list of genes, fold change and *p*-values were manually entered from the analysis group data sheet. The data was again imported into IPA and core analysis was performed without z-score and *p*-value cutoffs.

2.6.3 Selecting all networks with 'Cell Movement' as one of the Top Disease and Function

All the migration functions were selected from 'Diseases and Functions' tab and added to a new 'My Pathway' (used to build custom pathways). A set of genes without connections and directionality came up on which MAP (molecular activity predictor) overlay tool was applied to predict directionality effects. They were then overlaid with the information of the new dataset to get the observed expression of the genes in that dataset.

2.6.4 Building and overlaying

Nodes not in overlay dataset were trimmed and all the remaining molecules were connected using the build option. To filter the connections, only direct interactions and those observed in Humans were selected. To see the causal effect of the genes on migration function, the network was grown to selected functions and node connectivity greater than zero was kept, that is, orphans were removed. To obtain a gene distribution among subcellular levels, subcellular layout of presentation was selected. Since we are interested in studying the secreted markers, molecules only in extracellular space were retained. Those canonical pathways connecting the dataset genes to migration function were overlaid onto the network.

3 RESULTS AND DISCUSSION

AIM 1: To investigate the effect of microtumor size (hypoxic microenvironments), time and secretome on the emergence of migratory phenotype in otherwise non-migratory microtumors fabricated from the same parent cells

3.1 Tumor Models

As noted in section 2.1, microarray was run on two non-migratory and two migratory T47D microtumor models:

1) 150μm/day 6 (non-hypoxic/non-migratory)

2) 600μm/day 1 (non-hypoxic, non-migratory)

3) 600μm/day 6 (hypoxic, migratory)

4) 150μm/CM (non-hypoxic, yet migratory).

Gene expression profiles were then compared (**Table 1**) between non-migratory and migratory models to delineate effect of following factors on the emergence of migratory phenotype:

A) Time of progression (600μm/day 6 *vs.* 600μm/day 1);

B) Hypoxia generated by controlled microtumor size (600μm/day 6 *vs.*150μm/day 6);

C) Secretome (150/CM Day 6 *vs.*150μm/day 6)

Table 1: Analysis groups representing temporal, size or secretome effect on microtumor migration

Comparison	Depicts
600μm/Day 6 *vs.* 600μm/Day 1	Temporal effect
600μm/Day 6 *vs.* 150μm/Day 6	Size effect
150/CM Day 6 *vs.* 150μm/Day 6	Secretome effect

3.2 Hierarchical clustering of gene expression profiles

The microarray experiment was performed for triplicates of all the experimental groups, viz. 150µm/Day 6, 600µm/Day 1, 600µm/Day 6 and 150/CM Day 6. To ensure that the replicates of an experimental group have similar gene expression profile, hierarchical clustering was performed in TAC as shown in **Figure 8**. This identifies experimental groups that are clustered closest to each other in the dendrogram. Log2-transformed expression values were plotted in the heat map with blue being the lowest expression value and red being the highest.

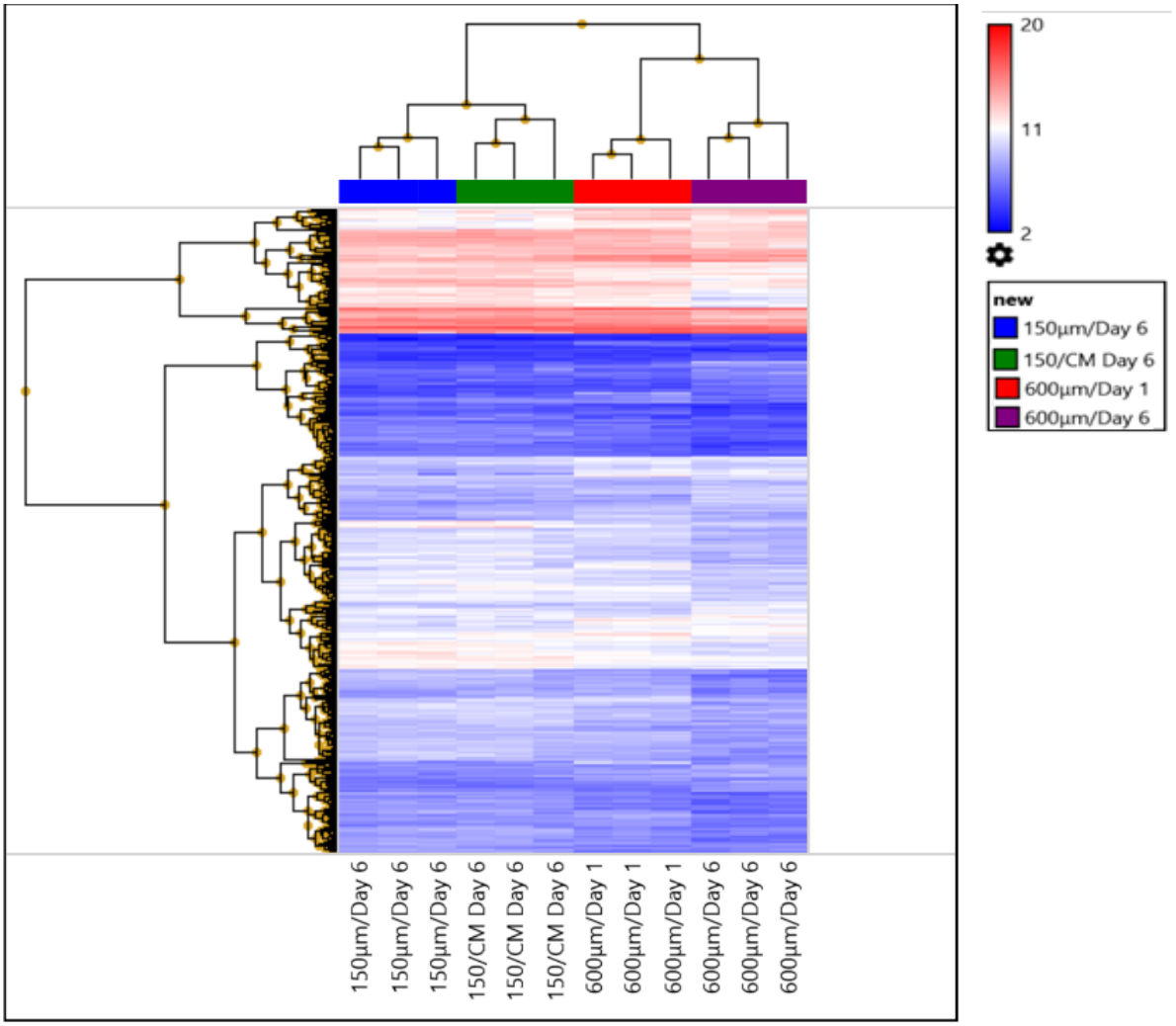

Figure 8: Hierarchical clustering of gene expression profiles of 150µm/Day 6, 600µm/Day 1, 600µm/Day 6 and 150/CM Day 6.

The values plotted are log2- transformed expression values.

It is evident from Figure 8 that replicates of each experimental group are clustered together confirming high similarity of gene expression profiles amongst replicates. After clustering of the replicates, small and large size microtumors are clustered together, that is, 150µm/Day 6 and 150/CM Day 6 are clustered together, and 600µm/Day 1 and 600µm/Day 6 are clustered together. This shows the dominant effect of the microtumor size on gene expression profiles, that is, irrespective of the time or secretome effect, same sized microtumors have similar gene expression

profiles. Despite the treatment with 600µm conditioned media (CM), 150/CM Day 6 was found to cluster together with 150µm/ Day 6 rather than 600µm/ Day 6.

To further understand the effects of microtumor size, time and secretome on the gene expression signatures driving microtumor migration and invasion, pathway and network analysis was performed in IPA.

3.3 Temporal effect on pathways and biological functions of migratory phenotype

Large (600µm) microtumors, did not migrate out of the microwells on day 1, but started migrating as early as day 3 and continued to migrate throughout the culture period of 6 days. Hence, to analyze the temporal dynamics of emergence of migratory phenotypes in large microtumors, large microtumors were harvested on day 1 (non-migratory) and day 6 (migratory). The differential mRNA expression between the two microtumor models, viz. 600µm/Day 6 and 600µm/Day 1, was analyzed to identify pathways that are significantly activated or inhibited as the large microtumors transition from non-migratory to migratory phenotypes over the period of 6 days. Differential gene expression between 600µm/Day 6 *vs.* 600µm/Day 1 represented as fold change and the statistical significance of the difference between the expression value represented as *p*-values of 600µm/Day 6 and 600µm/Day 1 comparison were obtained from TAC. Filter was applied on the fold change with absolute value greater than 2 and *p*-value greater than 0.05. Four hundred and fifty-seven genes were significantly upregulated in 600µm/Day 6 and 864 genes were significantly downregulated when compared to 600µm/Day 1. Two thousand eight hundred and eighty-seven genes had similar expression (absolute fold change was less than 2) in both the experimental groups. Core analysis was performed on the gene expression data imported into IPA. Fold change was used as the base of measurement.

Figure 9 shows the top canonical pathways with *p*-value less than 0.001 and absolute z-score greater than 0.1. Orange color denotes activation of the pathways while blue color denotes their inhibition. Cholesterol biosynthesis pathways are significantly downregulated while ATM (ATM serine/threonine kinase) signaling pathway is upregulated in 600µm/Day 6 group as compared to 600µm/Day 1. In many cancers, like prostate cancer, cholesterol biosynthesis pathways are known to be downregulated as cholesterol synthesis is an energy intensive process and cancer cells tend to downregulate such processes.[83] It is reported that ATM signaling is activated in response to physiological stress conditions such as hypoxia.[84] Activated ATM signaling pathway is known to upregulate the cell cycle checkpoint pathways such as p53 signaling and G2/M DNA damage checkpoint regulation[85-86] which is observed in **Figure 9**. The sirtuin signaling pathway is reported to be crucial in cell survival under stress.[87] Interferon signaling pathway is an important tumor-suppressive pathway and is known to activate cell proliferation, and survival related biological functions.[88-89] From the canonical pathways, we can infer that hypoxic conditions prevail in large tumors by day 6.

Figure 9: Analysis to identify top pathways affected by the microtumor size using migratory 600µm/Day 6 *vs.* non-migratory 600µm/Day 1

Top Canonical pathways derived from Core analysis in Ingenuity Pathway Analysis with -log(*p*-value) greater than 3 and absolute z-score greater than 0.1

To obtain the list of genes that are resultant of hypoxic conditions, 600µm/Day 6 *vs.* 600µm/Day 1 dataset was compared to the list of genes downstream of hypoxia obtained from IPA Knowledgebase, the result of which is shown in **Table 2**.

Table 2: Genes common between 600µm/Day 6 *vs*. 600µm/Day 1 and genes resultant of hypoxic condition obtained from IPA knowledgebase
CA5B, CA9, MB, NR3C1, PARK7, PDE8A, SLC7A11, TMEM38B, VEGFA

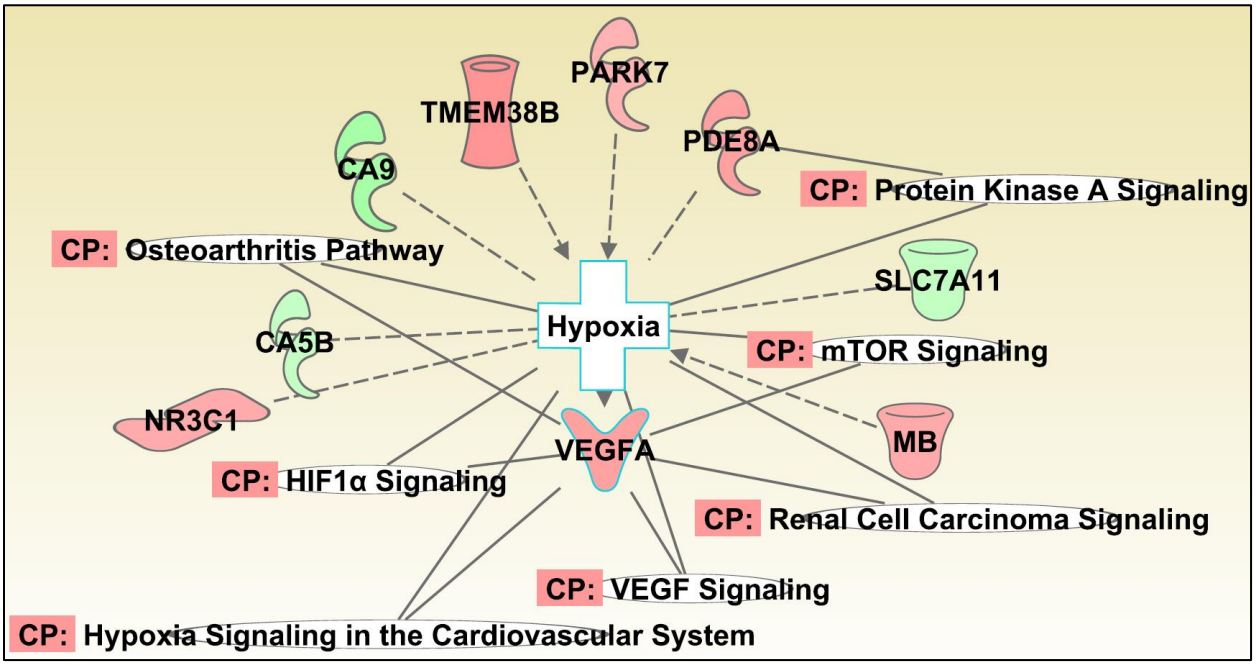

Figure 10: Relation between Hypoxia function and genes affecting hypoxia in 600µm/Day 6 *vs*. 600µm/Day 1 dataset

Canonical pathways (CP) connecting hypoxia and the genes are also presented. Genes that are upregulated are in red nodes and ones that are downregulated are in green nodes, the intensity of which is determined by the fold change of the genes. Genes in uncolored nodes are not a part of our gene dataset. Predicted activation of genes is shown as orange node while predicted inhibition is shown as blue nodes. Solid lines represent direct relationship and dotted lines represent indirect relationship.

Figure 10 shows that hypoxia causes upregulation of *VEGFA* through multiple pathways, viz., VEGF signaling, hypoxia signaling in the cardiovascular system, renal cell carcinoma signaling, HIF1α signaling, osteoarthritis pathway and mTOR signaling. Hypoxia also has effect on *CA5B*

(carbonic anhydrase 5B), *CA9* (carbonic anhydrase IX), *NR3C1* (nuclear receptor subfamily 3 group c member 1), *SLC7A11* (solute carrier family 7 member 11), and *PDE8A* (phosphodiesterase 8A) genes. *MB* (myoglobin)[90-91], *TMEM38B* (transmembrane protein 38B)[92], and *PARK7* (parkinsonism associated deglycase)[93] genes regulate hypoxic conditions.

Cellular movement comes up as a statistically significant Disease/Bio function (p-value<0.01). To understand the precise effect of those genes whose expression is significantly different in migratory 600µm/Day 6 from non-migratory 600µm/Day 1 on migration function, the gene dataset was compared to 'migration of cells' function dataset obtained from the IPA Knowledgebase. This resulted in 221 genes that directly or indirectly affect migration function.

Core analysis of those 221 genes gave upstream regulators that are responsible for the observed gene expression. *RARB* (retinoic acid receptor beta), and *BRD4* (bromodomain-containing protein 4) are two of these upstream regulators that have direct or indirect effect on the 'migration of cells' function. Both the genes have predicted downregulation in 600µm/Day 6 group as compared to 600µm/Day 1. **Figure 11** shows directional effect of upstream regulators *BRD4* and *RARB* on migration of endothelial cells and migration of tumor cell lines functions respectively via dataset genes of 600µm/Day 6 *vs*. 600µm/Day 1 group. Legend indicates corresponding nodal shapes and nodal types.

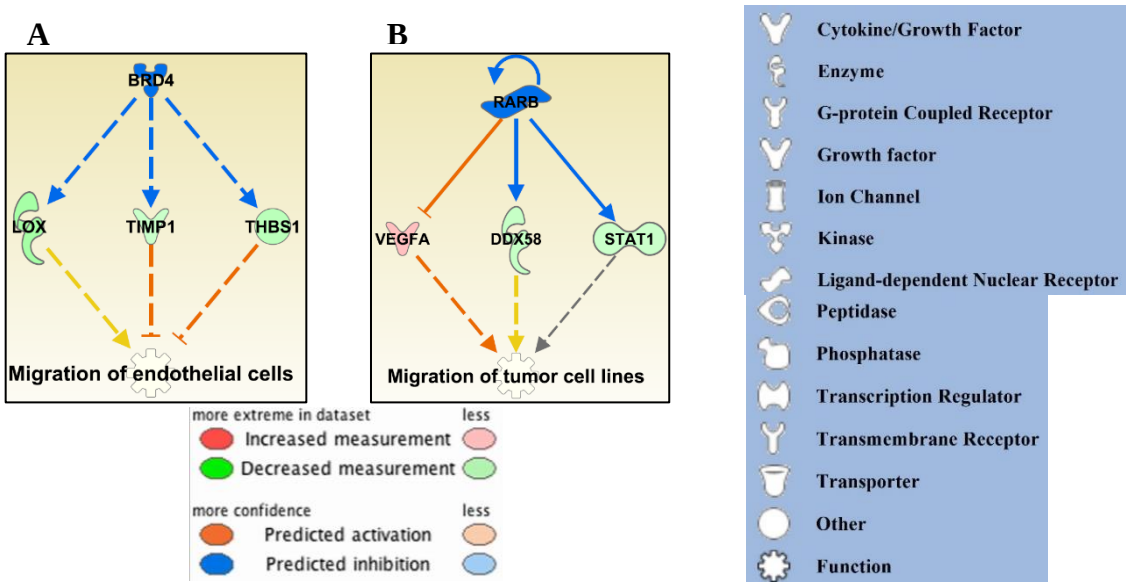

Figure 11: Directional effect of upstream regulators *BRD4* and *RARB* on migration functions via dataset genes 600µm/Day 6 *vs*. 600µm/Day 1

Legend indicates corresponding nodal shapes and nodal types. Genes that are upregulated are in red nodes and ones that are downregulated are in green nodes, intensity of which is determined by the fold change of the genes. Predicted activation of genes is shown as orange node while predicted inhibition is shown as blue nodes. Solid lines represent direct relationship and dotted lines represent indirect relationship. Orange interaction line represents function activation due to the gene and blue line indicates the inhibition of function. Yellow lines indicate that fold change value inconsistent with literature and grey lines indicate findings not predicted in literature.

It is reported that *RARB* reduces migration of human breast cancer cells (MCF7 and T47D)[94] as seen in **Figure 11**. Studies have shown that *BRD4* inhibition suppresses migration of HUVECS (human umbilical vein endothelial cells)[95] and idiopathic pulmonary fibrosis lung fibroblasts[96] which is inconsistent with our findings.

The genes were sorted into subcellular levels depending on their location as reported in literature. Since we are interested in studying the secreted markers, genes that showed up in the extracellular space in the subcellular layout were filtered. The genes were grown to connect to 'Migration of

cells' function followed by overlaying all the canonical pathways (CP) containing migration of cells function and the dataset genes. **Figure 12** shows the network between migration of cells function, extracellular molecules from the dataset and the canonical pathways through which the molecules affect the function.

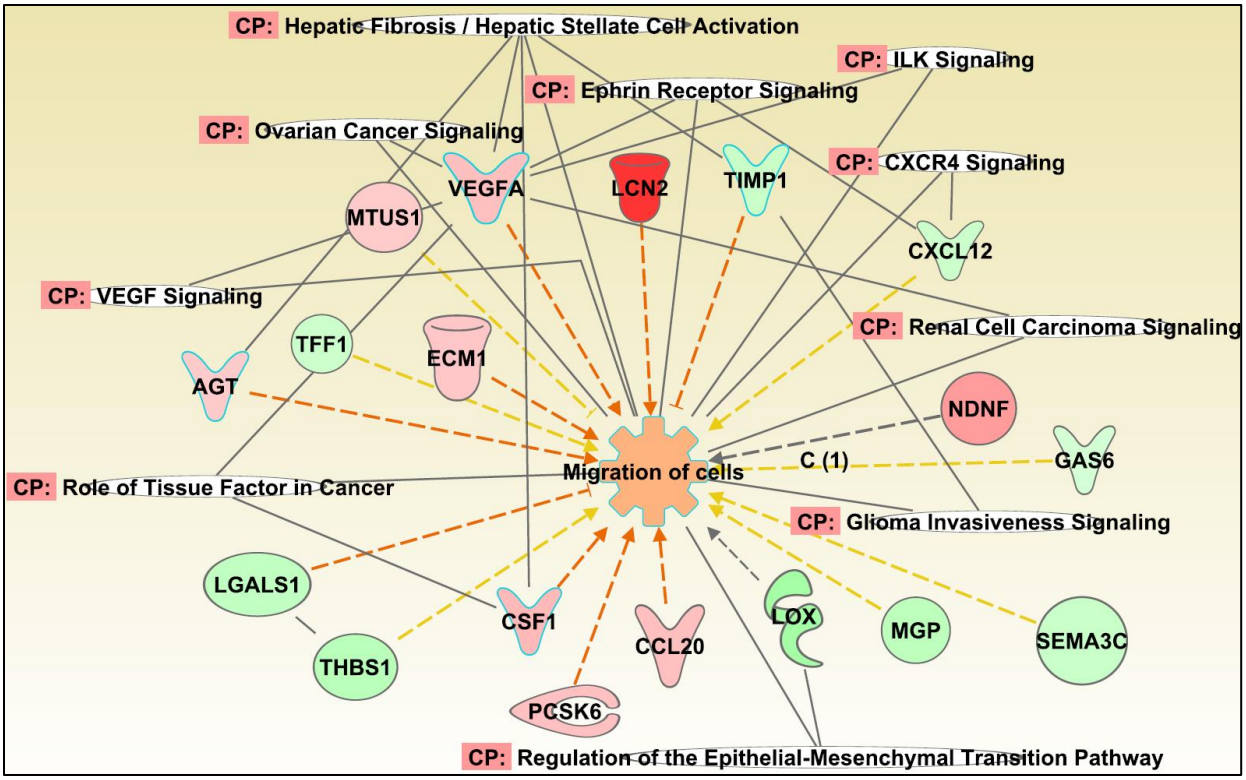

Figure 12: Network of extracellular molecules from the 600µm/Day 6 *vs*. 600µm/Day 1 dataset and the 'migration of cells' function including the canonical pathways through which the interaction between genes and function occurs.

Legend shows which nodal shape corresponds to which node type. Genes that are upregulated are in red nodes and ones that are downregulated are in green nodes, intensity of which is determined by the fold change of the genes. Predicted activation of genes is shown as orange node while predicted inhibition is shown as blue nodes. Solid lines represent direct relationship and dotted lines represent indirect relationship. Orange interaction line represents function activation due to the gene and blue line indicates the inhibition of function. Yellow lines indicate that fold change value inconsistent with literature and grey lines indicate findings not predicted in literature.

Thus, time effect led to elevated expression of many genes represented by red nodes in **Figure 12**. *VEGFA* affects migration function through 'role of tissue factor in cancer', 'ILK signaling', 'ephrin receptor signaling', 'renal cell carcinoma signaling', 'VEGF signaling', 'ovarian cancer signaling', and 'hepatic fibrosis/hepatic stellate cell activator' pathways while *CXCL12* affects via 'CXCR4 signaling', and 'ephrin receptor signaling' pathways. *AGT* acts through 'hepatic fibrosis/hepatic stellate cell activator' pathway, *CSF1* through 'hepatic fibrosis/hepatic stellate cell activator', and 'role of tissue factor in cancer' pathways, *TIMP1* through 'glioma invasiveness signaling', and 'hepatic fibrosis/hepatic stellate cell activator' pathways, and *LOX* through 'regulation of the epithelial-mesenchymal transition pathway' to affect the migration function.

It should be noted that the extracellular molecules highly expressed in our migratory large microtumors, namely, *PCSK6*(proprotein convertase subtilisin/kexin type 6)[97], *LCN2* (lipocalin 2)[98], *AGT* (angiotensinogen)[99], *CSF1* (colony stimulating factor 1)[100], *VEGF* (vascular endothelial growth factor)[101], *ECM1* (extracellular matrix protein 1)[102], *CCL20* (chemokine (c-c motif) ligand 20)[103] have already been reported to affect breast cancer migration while no concrete literature exists suggesting direct effect of *NDNF* (neuron derived neurotrophic factor) and *MTUS1* (mitochondrial tumor suppressor 1) genes in our dataset on breast cell migration. Out of these extracellular molecules shown in **Figure 12**, many have been reported to be a product of hypoxic conditions, *viz.*, *VEGFA*[104], *LCN2*[105], *AGT*[106], *CSF1*[107], *CCL20*[108]. This indicates that there might be hypoxic conditions in 600μm/Day 6 tumors which resulted in genes triggering migration. Note that some of these hypoxia related genes are not shown in **Figure 10** due to the limitations of IPA Knowledgebase. Like other bioinformatics software, IPA too does not cover the entire literature available for a condition.

3.4 Effect of microtumor size (hypoxia) on pathways and biological functions

Although fabricated from the same parent T47D breast cancer cells, small (150µm) microtumors remain non-migratory over 6 days in culture while large (600µm) microtumors show emergence of migratory phenotype starting as early as day 3. Differential gene expression profiles of these two microtumor models both harvested on day 6, viz., 600µm/Day 6 and 150µm/Day 6, were then studied to provide an insight into the gene signature responsible for migration of cells. To further investigate the functions affected significantly in migratory 600µm *vs*. non-migratory 150µm microtumors, differential gene expression between 600µm/Day 6 *vs.* 150µm/Day 6 represented as fold change and the significance of the difference between the expression value represented as *p*-value were obtained by importing the raw data files of the experimental groups into TAC. The genes showing absolute fold change value greater than 2 and *p*-value less than 0.05 were selected for analysis. One thousand two hundred and fifty-eight genes were significantly downregulated, and 700 genes were significantly upregulated in 600µm/Day 6 group when compared to 150µm/Day 6. Three thousand one hundred and fifty-three genes had similar expression in both the groups. The analyzed gene expression data was then imported into IPA. Expression core analysis was run where the analysis was based on the fold change measurement. Only molecules/relationships reported in humans were considered. Core Expression analysis produced relationship networks, activated pathways, affected biological functions and upstream regulators. Top canonical pathways with *p*-value less than 0.001 and absolute z-score greater than 0.1 are shown in **Figure 13**.

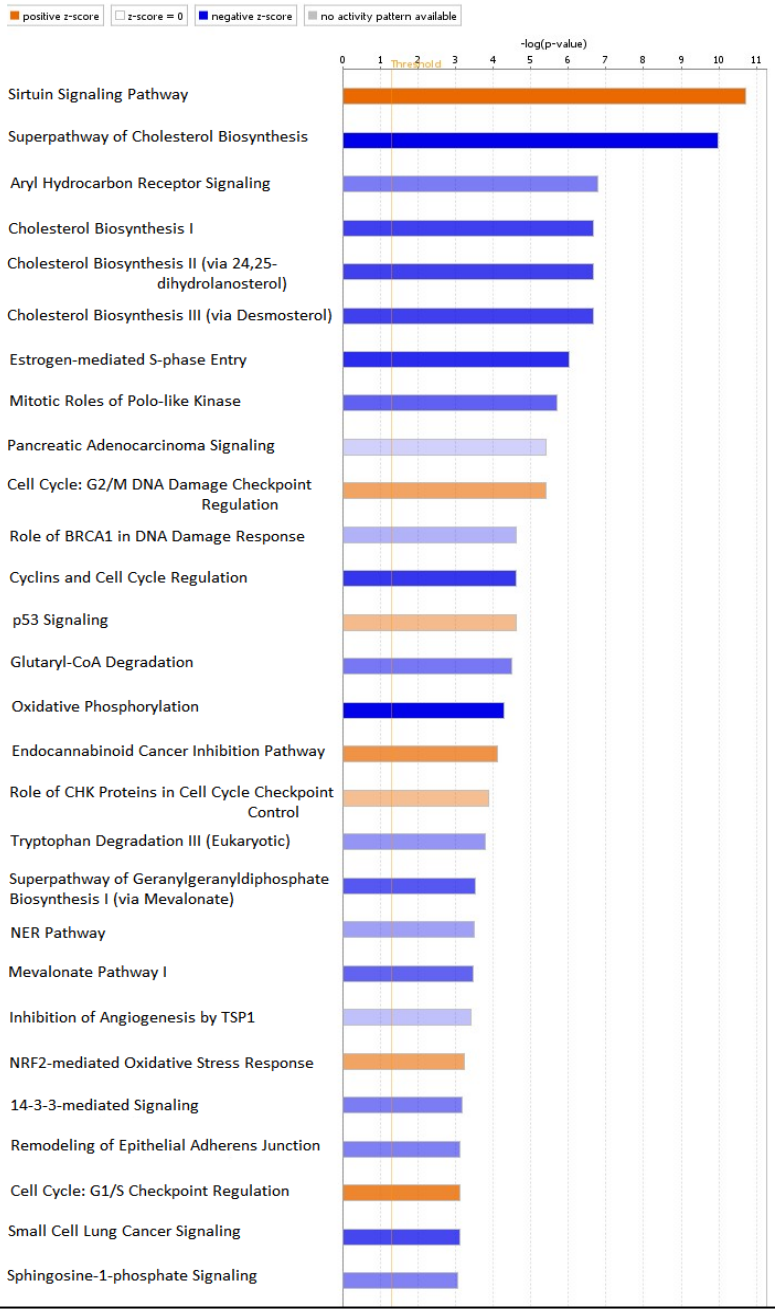

Figure 13: Analysis to identify top pathways affected by the microtumor size using migratory 600µm/Day 6 *vs*. non-migratory 150µm/Day 6

Top Canonical pathways derived from Core analysis in Ingenuity pathway analysis with -log(*p*-value) greater than 3 and absolute z-score greater than 0.1 functions.

The superpathway of cholesterol biosynthesis is highly significant with the lowest z-score (evident from intensity of the blue bar) and sirtuin signaling pathway is highly significant with highest z-

score in 600µm/Day 6 microtumor models. Like the 600µm/Day 6 *vs.* 600µm/Day 1 group, sirtuin signaling pathway and sterol synthesis pathways are among the top pathways in 600µm/Day 6 microtumor models when compared to 150µm/Day 6 microtumor models. Activated *p53* signaling pathways are known to induce cell cycle arrest, cell survival and apoptosis.[109] One of the reasons of *p53* activation is hypoxia. It is known to induce *p53* activation in oncogenically transformed cells.[110] In cell cycle regulation pathways, *p53* is a crucial gene whose activation is also triggered by *ATM, ATR* and *CHK2*. Hence activation of 'G2/M DNA damage checkpoint regulation', 'p53 signaling', 'role of CHK proteins in cell cycle checkpoint control', and 'G1/S checkpoint regulation' pathways is seen in **Figure 13**. 'NRF2-mediated oxidative stress response' was seen to be upregulated in hypoxic conditions in rat brain.[111] Hence, like the 600µm/Day 6 *vs.* 600µm/Day 1 group, hypoxia may be the reason for the predicted activation or inhibition of certain canonical pathways in 600µm/Day 6 *vs.* 150µm/Day 6 group. This shows that we successfully developed tumor models with hypoxic and non-hypoxic microenvironment by engineering tumor size.

To obtain the list of genes that are resultant of hypoxic conditions, 600µm/Day 6 *vs.* 600µm/Day 1 dataset was compared to list of genes downstream of hypoxia obtained from IPA Knowledgebase, the result of which is shown in **Table 3**.

Table 3: Genes common between 600µm/Day 6 *vs.* 150µm/Day 6 and genes resultant of hypoxic condition obtained from IPA knowledgebase
CA12, CA9, COMT, DLL4, GNAI2, MB, PARK7, VEGFA

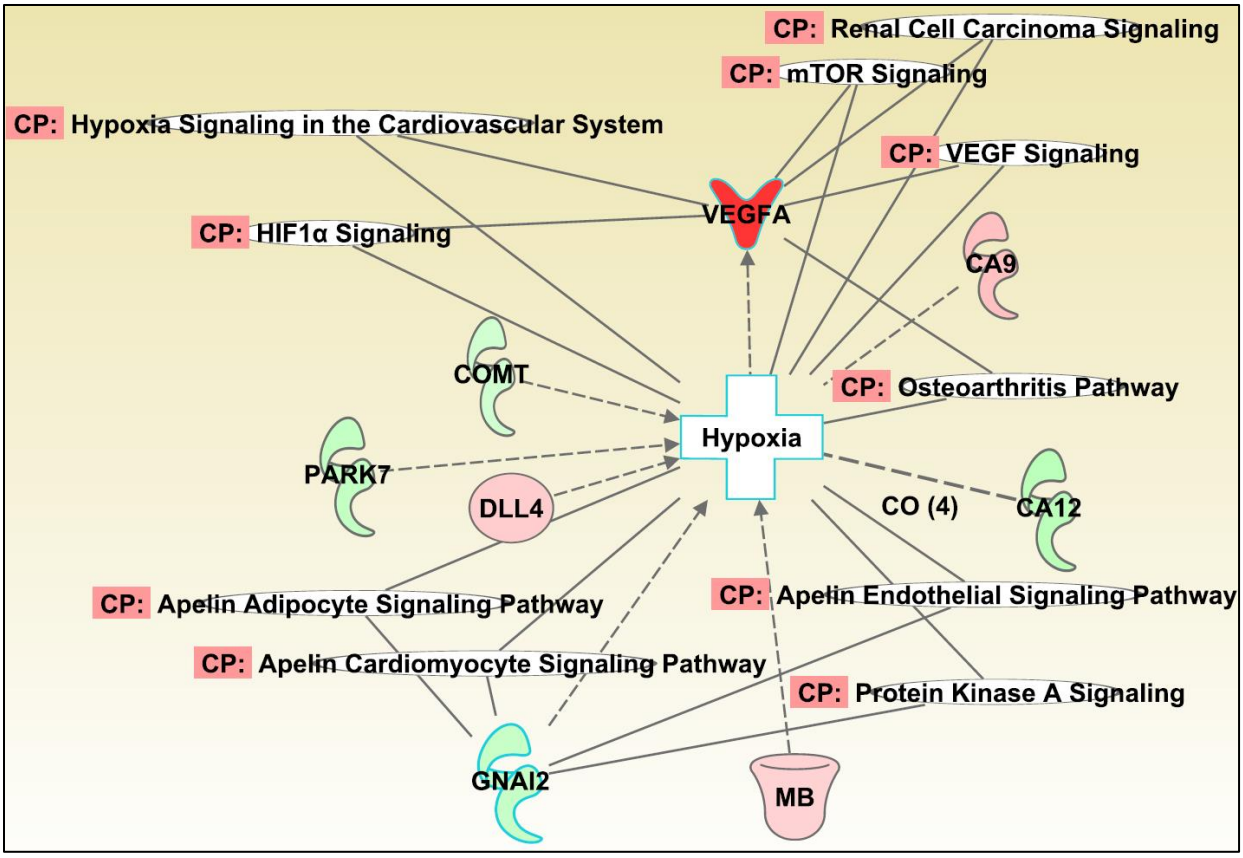

Figure 14: Relation between Hypoxia function and genes affecting hypoxia in 600µm/Day 6 *vs.* 150µm/Day 6 dataset

Canonical pathways (CP) connecting hypoxia and the genes are also presented.

Legend shows which nodal shape corresponds to which node type. Genes that are upregulated are in red nodes and ones that are downregulated are in green nodes, intensity of which is determined by the fold change of the genes. Predicted activation of genes is shown as orange node while predicted inhibition is shown as blue nodes. Solid lines represent direct relationship and dotted lines represent indirect relationship.

Figure 14 shows the relationship between hypoxia function and genes affecting hypoxia in 600µm/Day 6 *vs.* 150µm/Day 6 dataset. Like 600µm/Day 6 *vs.* 150µm/Day 6 group, hypoxia causes upregulation of *VEGFA* through multiple pathways, viz., VEGF signaling, Hypoxia signaling in the cardiovascular system, Renal cell carcinoma signaling, HIF1α signaling,

osteoarthritis pathway and mTOR signaling. *GNA12* (G protein subunit alpha 12) expression is affected by hypoxia via protein kinase A signaling, apelin cardiomyocyte signaling pathway, apelin adipocyte signaling pathway, and apelin endothelial signaling pathway. Hypoxia also has effect on *CA12* (carbonic anhydrase 12), and *CA9* genes. *MB* [90-91], *COMT* (catechol-O-methyltransferase)[112], *DLL4* (delta-like protein 4)[113], and *PARK7*[93] genes regulate hypoxic conditions. Out of these genes, *MB, PARK7, VEGFA*, and *CA9* are affected or affect hypoxia as a result of both time effect and presence of hypoxic microenvironments (size effect).

Cellular movement comes up as a statistically significant Disease/Bio function with *p*-value less than 0.01. To further understand the processes involved in the emergence of the microtumor migration, our gene dataset was compared to 'migration of cells' function dataset obtained from the IPA Knowledgebase. This resulted in 351 genes that directly or indirectly affect migration function. Core analysis of those 351 genes gave upstream regulators that are responsible for the observed gene expression as shown in **Figure 15**.

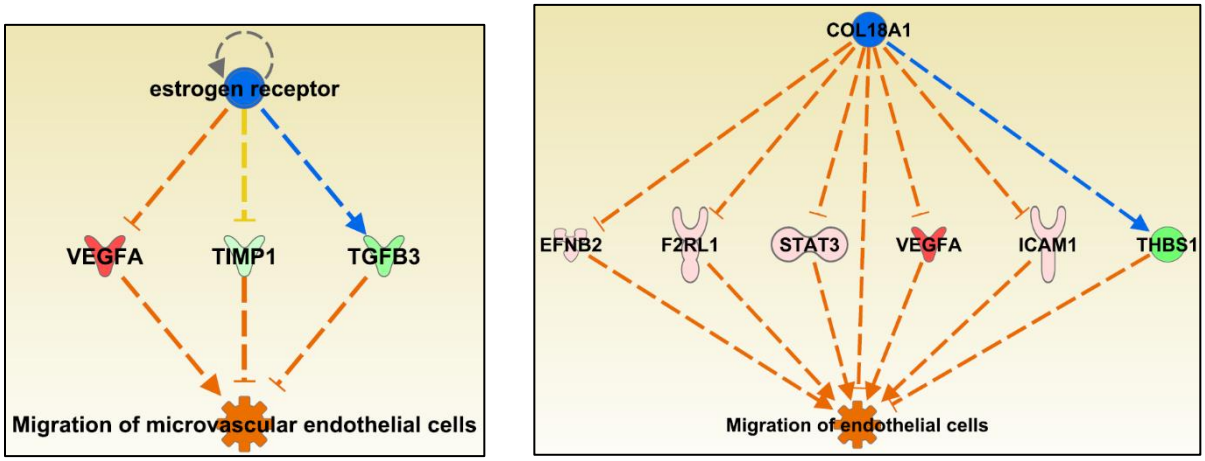

Figure 15: Directional effect of upstream regulators *COL18A1* and *ER* on migration functions via dataset genes 600µm/Day 6 *vs*. 150µm/Day 6

Legend shows which nodal shape corresponds to which node type. Genes that are upregulated are in red nodes and ones that are downregulated are in green nodes, intensity of which is determined by the fold change of the genes. Predicted activation of genes is shown as orange node while predicted inhibition is shown as blue nodes. Solid lines represent direct relationship and dotted lines represent indirect relationship. Orange interaction line represents function activation due to the gene and blue line indicates the inhibition of function. Yellow lines indicate that fold change value inconsistent with literature and grey lines indicate findings not predicted in literature.

COL18A1 (collagen type XVIII alpha 1 chain), and *ER* (estrogen receptor) are two of these upstream regulators that have direct or indirect effect on the 'migration of cells' function. Studies have shown that *COL18A1* is responsible for suppression of migration of endothelial cells.[114-115] Estrogen receptor regulates differential expression of *VEGFA*, *TIMP1*, and *TGFB3* which results in activation of 'migration of microvascular endothelial cells' function while *COL18A1* regulates *EFNB2*, *F2RL1*, *STAT3*, *VEGFA*, *ICAM1*, AND *THBS1* who intern activate 'migration of endothelial cells' function.

To study the secreted markers, genes that showed up in the extracellular space in the subcellular layout were filtered. The genes were grown to connect to ‘Migration of cells’ function followed by overlaying all the canonical pathways (CP) containing migration of cells function and the dataset genes. **Figure 16** shows the network between migration of cells function, extracellular molecules from the dataset and the canonical pathways through which the molecules affect the function.

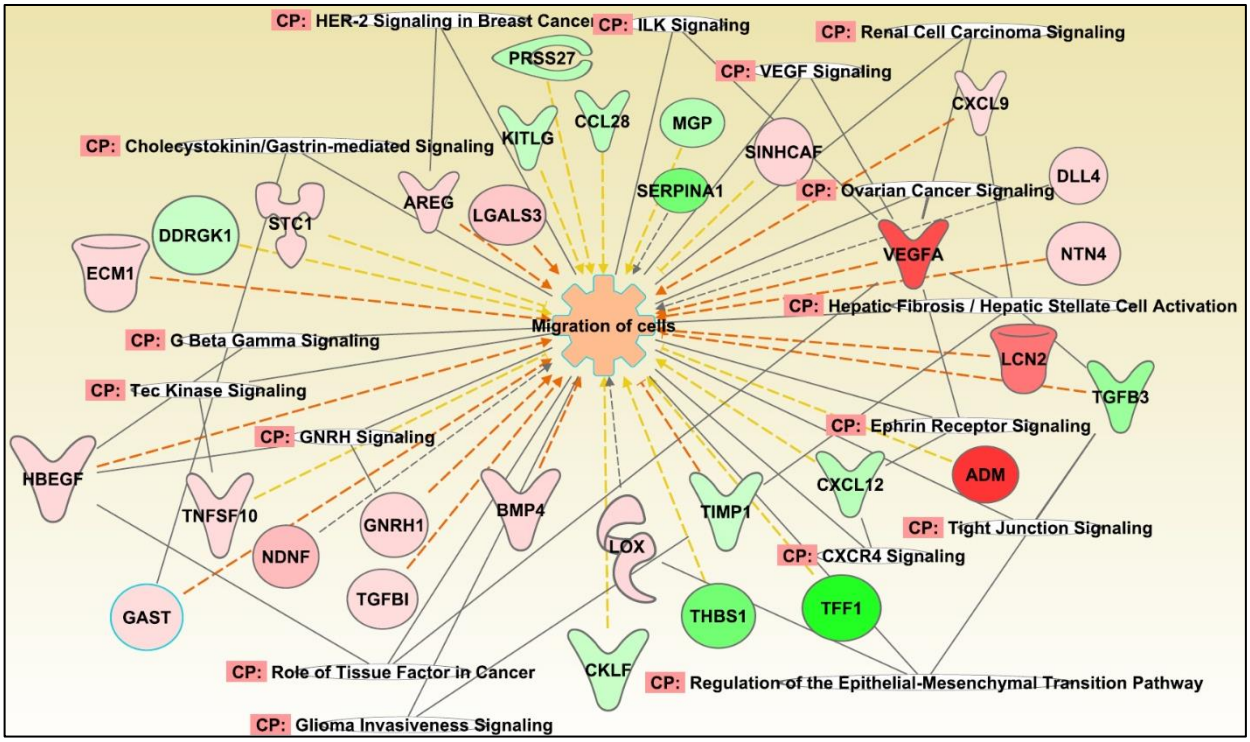

Figure 16: Network of extracellular molecules from the 600µm/Day 6 *vs.* 150µm/Day 6 dataset and the 'migration of cells' function including the canonical pathways through which the interaction between genes and function occurs

Legend shows which nodal shape corresponds to which node type. Genes that are upregulated are in red nodes and ones that are downregulated are in green nodes, intensity of which is determined by the fold change of the genes. Predicted activation of genes is shown as orange node while predicted inhibition is shown as blue nodes. Solid lines represent direct relationship and dotted lines represent indirect relationship. Orange interaction line represents function activation due to the gene and blue line indicates the inhibition of function. Yellow lines indicate that fold change value inconsistent with literature and grey lines indicate findings not predicted in literature.

Figure 16 shows that with increase in size, migration pattern also changes. Controlled modulation of microtumor size resulted in upregulation of *LGALS3* (galectin 3), *LOX* (lysyl oxidase), *ADM* (adrenomedullin), *VEGF*, *HBEGF* (heparin-binding EGF-like growth factor), *CXCL9* (chemokine (c-x-c motif) ligand 9), *AREG* (amphiregulin), *LCN2*, *BMP4* (bone morphogenetic protein 4), *TNFSF10* (tumor necrosis factor (ligand) superfamily, member 10), *GAST* (gastrin), *DLL4*, *ECM1*, *STC1* (stanniocalcin-1), *TGFB1* (transforming growth factor beta 1) extracellular genes as represented with red nodes in **Figure 16**. *VEGFA* affects migration function through 'role of tissue factor in cancer', 'ILK signaling', 'ephrin receptor signaling', 'renal cell carcinoma signaling', 'VEGF signaling', 'ovarian cancer signaling', and 'hepatic fibrosis/hepatic stellate cell activator' pathways while *TIMP1* acts through 'glioma invasiveness signaling', and 'hepatic fibrosis/hepatic stellate cell activator' pathways, and *LOX* through 'regulation of the epithelial-mesenchymal transition pathway' to affect the migration function. *TGFB3* acts through 'tight junction signaling', and 'regulation of the epithelial-mesenchymal transition pathway', *CXCL9* through 'hepatic fibrosis/hepatic stellate cell activator' pathway, and *GAST* through 'cholecystokinin/gastrin mediated signaling' pathway to affect migration function. This function is also affected by *GNRH1* through 'GNRH signaling' pathway, *TNFSF10* through 'tec kinase signaling', *HBEGF* through 'role of tissue factor in cancer', 'beta gamma signaling', and 'GNRH signaling' pathways, and *AREG* through 'HER-2 signaling in breast cancer' pathway.

Indeed, *LOX*[116], *VEGF*[101], *HBEGF*[117], *LCN2*[98], *BMP4*[118], *DLL4*[119], *ECM1*[102], *STC1*[120], *TGFB1*[121], *LGALS3*[122], and *AREG*[123] have been implicated in promoting breast cancer migration, which further validates observations in our microtumor models. However, effects of *ADM*, *CXCL9*, *TNFSF10*, *GAST* molecules on breast cancer migration are clearly stated and warrants further investigation. Out of these extracellular molecules shown in **Figure 16,** many have been reported

to be a product of hypoxic conditions, *viz.*, *LOX*[124], *VEGFA*[104], *LCN2*[105], *HBEGF*[125], *BMP4*[126], *DLL4*[127], *STC1*[128], *TGFB1*[129].

Both, 600µm/Day 6 *vs.* 600µm/Day 1 and 600µm/Day 6 *vs.* 150µm/Day 6 represent elevated hypoxia and increased migration due to the temporal and size effect, respectively. *VEGFA, LCN2, ECM1* were common extracellular molecules, all of which are downstream of hypoxia, suggesting that these extracellular molecules are upregulated in a time-dependent and microtumor size-dependent manner. But there are molecules which are elevated in one of the two groups; *PCSK6, AGT, CSF1, CCL20, NDNF* and *MTUS1* genes' elevated expression is solely the result of temporal effect and *LGALS3, LOX, ADM, HBEGF, CXCL9, AREG, BMP4, TNFSF10, GAST, DLL4, STC1, TGFB1* genes' elevated expression is solely the result of size effect.

3.5 Effect of secretome (conditioned media of large microtumors, 600/CM) on migration of once non-migratory group

We hypothesize that factors secreted by the migratory microtumors (secretome) have potential to induce migration and/or invasion in non-migratory microtumors. To test this hypothesis, non-migratory, non-hypoxic small (150µm) microtumors were treated with conditioned media from large (600µm) microtumors (600/CM) everyday once they start migrating from day 3 onwards. Interestingly, on day 6, the once non-migratory small microtumors treated with the 600/CM started migrating out of the microwells. These small non-hypoxic yet migratory microtumor models are referred as '150/CM'. The emergence of the migratory phentoype in response to the added 600/CM suggests the role of tumor secreted factors such as chemokines, cytokines, etc. (secretome) in driving migration. To delineate the effect of secretome on the gene expression and pathway activation, gene expression of non-hypoxic, yet migratory 150/CM Day 6 was compared with that

of non-hypoxic, non-migratory 150µm/Day 6 in order to obatin secretome-specific signature of microtumor migration. Note that in both the microtumor models (150/CM Day 6 and 150µm/Day 6), microtumor size and hence, hypoxic status and time of culture was kept contant; thus, migratory signaure could be attributed solely to the secretome effect.

To understand the functions affected significantly in non-hypoxic, yet migratory 150/CM *vs*. non-hypoxic, non-migratory 150µm microtumors, both harvested on day 6, differential gene expression between 150/CM Day 6 *vs.* 150µm/Day 6 represented as fold change and the significance of the difference between the expression value represented as *p*-values were obtained by importing the raw data files of the experimental groups into TAC. The genes showing absolute fold change value greater than 2 and *p*-value less than 0.05 were selected for analysis. One hundred and eighty-seven genes were significantly upregulated, and 137 genes were significant downregulated in 150/CM Day 6. One thousand seven hundred and ninety-six genes had similar expression in both the groups.

Core analysis was performed in IPA without any z-score and *p*-value cutoffs, which resulted in top canonical pathways with -log(*p*-value) greater than 1.3 and absolute z-score greater than 0.1 as shown in **Figure 17**.

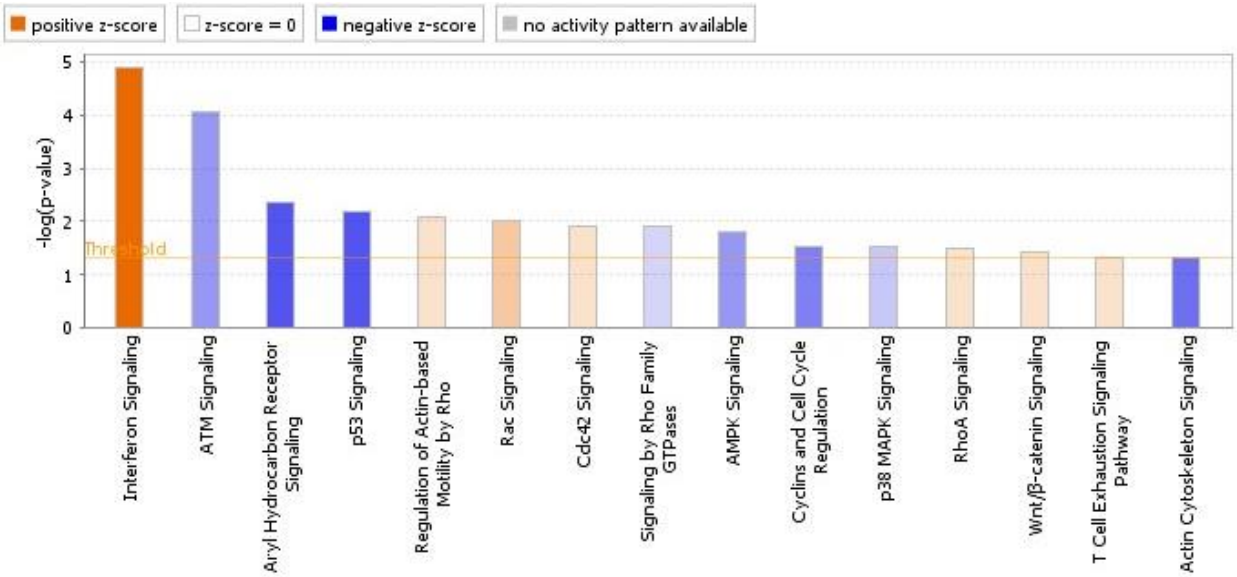

Figure 17: Analysis to identify top pathways affected by the secretome using migratory 150/CM Day 6 *vs.* non-migratory150µm/Day 6

Top Canonical pathways derived from Core analysis in Ingenuity pathway analysis with -log(*p*-value) greater than 1.3 and absolute z-score greater than 0.1

Unlike 600µm/Day 6 *vs.* 150µm/Day 6 and 600µm/Day 6 *vs.* 600µm/Day 1 analysis groups discussed above (section 3.4 and 3.5, respectively), comparison between 150/CM Day 6 and 150µm/Day 6 microtumor models revealed no significant effect on the cholesterol biosynthesis pathways. Similarly, p53 and ATM signaling pathways were also downregulated in 150/CM Day 6 *vs.* 150µm/Day 6 microtumor models in contrast to their upregulation in 600µm/Day 6 *vs.* 150µm/Day 6 and 600µm/Day 6 *vs.* 600µm/Day 1. As mentioned in section 3.5, hypoxia activates p53, AMPK, RhoA and ATM signaling. Hence, downregulation of p53, AMPK, RhoA and ATM signaling in 150/CM Day 6 group might indicate absence of hypoxia. Upregulation of regulation of actin-based motility by Rho pathway leads to cell spreading and migration[130] as is depicted in the pathway. Upregulation of RAC is known to upregulate *CDC42* and *RhoA*[131]. Interestingly, Interferon signaling was significantly upregulated in 150/CM Day 6 *vs.* 150µm/Day 6 with the

highest z-score. Therefore, stress induced pathways were significantly downregulated due to secretome effect i.e. secretome of hypoxic tumors do not induce stress related pathways and migration related pathways were upregulated.

When compared to 150µm/Day 6 microtumors, 'Cellular movement' was top 3 network functions significantly affected in 150/CM Day 6 group. To obtain the list of genes that are resultant of hypoxic conditions, 150/CM Day 6 *vs*. 150µm/Day 6 dataset was compared to list of genes downstream of hypoxia obtained from IPA Knowledgebase. It is important to note that no genes showed up common between the two set of genes, which indicates the lack of hypoxic conditions and hence, its resultant downstream genes in 150/CM Day 6 group.

Our gene dataset was compared to 'migration of cells' function dataset obtained from the IPA Knowledgebase to understand the processes involved in the emergence of the migratory phenotype in response to the secretome treatment. This resulted in 65 genes that directly or indirectly affect migration function. To study the secreted markers, genes that showed up in the extracellular space in the subcellular layout were filtered. The genes were grown to connect to 'Migration of cells' function followed by overlaying all the canonical pathways containing migration of cells function and the dataset genes. **Figure 18** shows the network between migration of cells function, extracellular molecules from the dataset and the canonical pathways through which the molecules affect the function.

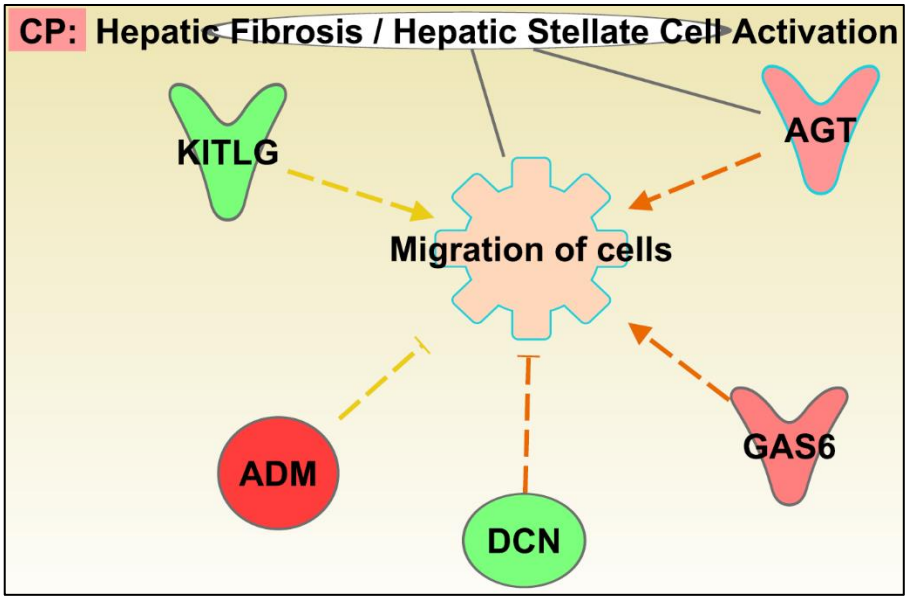

Figure 18: Network of extracellular molecules from the 150/CM Day 6 *vs*. 150µm/Day 6 dataset and the 'migration of cells' function including the canonical pathways through which the interaction between genes and function occurs

Legend shows which nodal shape corresponds to which node type. Genes that are upregulated are in red nodes and ones that are downregulated are in green nodes, intensity of which is determined by the fold change of the genes. Predicted activation of genes is shown as orange node while predicted inhibition is shown as blue nodes. Solid lines represent direct relationship and dotted lines represent indirect relationship. Orange interaction line represents function activation due to the gene and blue line indicates the inhibition of function. Yellow lines indicate that fold change value inconsistent with literature and grey lines indicate findings not predicted in literature.

Figure 18 shows that the secretome of large, migratory, tumors affect the migration of small, once non-migratory, tumors. Secretome effect resulted in upregulation of *GAS6, AGT, ADM* extracellular molecules that affect migration. *AGT* acts through 'hepatic fibrosis/hepatic stellate cell activator' pathway to affect migration function. Of these genes, *AGT*[99] has been reported to affect migration of breast cancer while *GAS6* and *ADM* have not been reported in literature. *AGT*

molecule is upregulated due to both time and secretome effect while *ADM* is upregulated in both size and secretome effect.

In conclusion, no hypoxic markers (as per IPA Knowledgebase) were detected in 150/CM Day 6 *vs.* 150μm/Day 6 group. Also, the canonical pathways showed opposite activation of cholesterol biosynthesis pathways, p53, AMPK, RhoA and ATM signaling pathways in 150/CM Day 6 *vs.* 150μm/Day 6 group when compared to the other two groups presented in section 3.4 and 3.5. *AGT* was commonly upregulated due to temporal (section 3.4) and secretome effect and *ADM* was commonly upregulated due to size (section 3.5) and secretome effect. The uncommon molecules might be a result of the time, size of tumor and secretome effect.

AIM 2: To investigate genes responsible for the difference in migratory behavior between large hypoxic and migratory tumors and small non-hypoxic yet migratory tumors.

3.6 Comparison of the migratory signature between secretome-induced migration (150/CM Day 6) and hypoxia-induced migration (600µm/Day 6)

As mentioned in section 1.5, large microtumors led to hypoxic microenvironment and migratory phenotype starting from day 3 (600µm/Day 6). Similarly, treatment with conditioned media of large microtumors also induced migratory phenotype in otherwise non-hypoxic and non-migratory small microtumors (150/CM Day 6). However, we observed differences in the migratory pattern between 600µm/Day 6 and 150/CM Day 6 as shown in **Figure 19A** and **B**. Large hypoxic (600µm) microtumors exhibited directionality while migrating, whereas secretome-induced migration in 150/CM did not show any directionality. We hypothesized that such differences could be attributed to the differences in gene expression and thus, mechanisms driving the migratory phenotype.

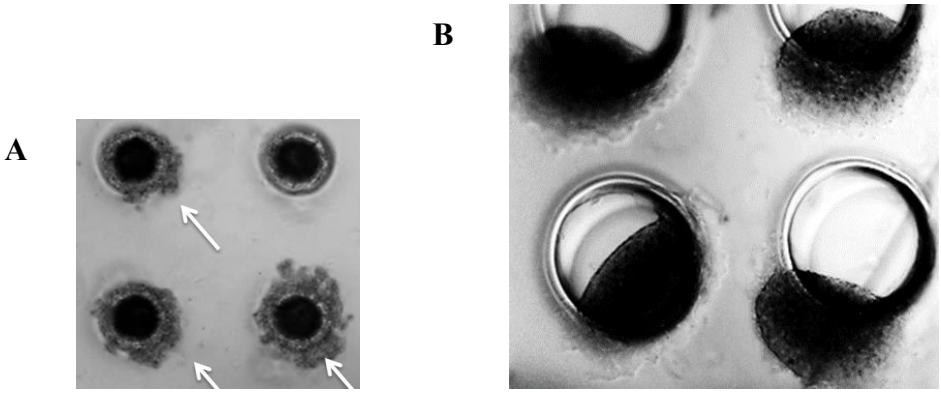

Figure 19: Different migratory pattern of A) 150/CM and B) 600µm microtumors on Day 6[75]

Log-2 transformation of mean expression values for each ID of replicates of 150/CM Day 6 and 600µm/Day 6 groups was carried out. The .CSV (comma separated values) file of the resultant data was imported in SAS 9.4 software. The SAS dataset was stored in a temporary file. Box plot was constructed using BOXPLOT function. INSETGROUP function was used to obtain summary statistics of each group. The SAS program used to obtain the box plot is as follows.

```
TITLE 'BOXPLOT OF LOG-2 TRANSFORMED MEAN EXPRESSION VALUES OF 600µm/Day 6
AND 150/CM Day 6';
PROC BOXPLOT DATA=MigratoryPattern;
PLOT Log2_ExpressionValue * Group;
INSETGROUP MIN MAX Q1 Q3 MEAN;
RUN;
```

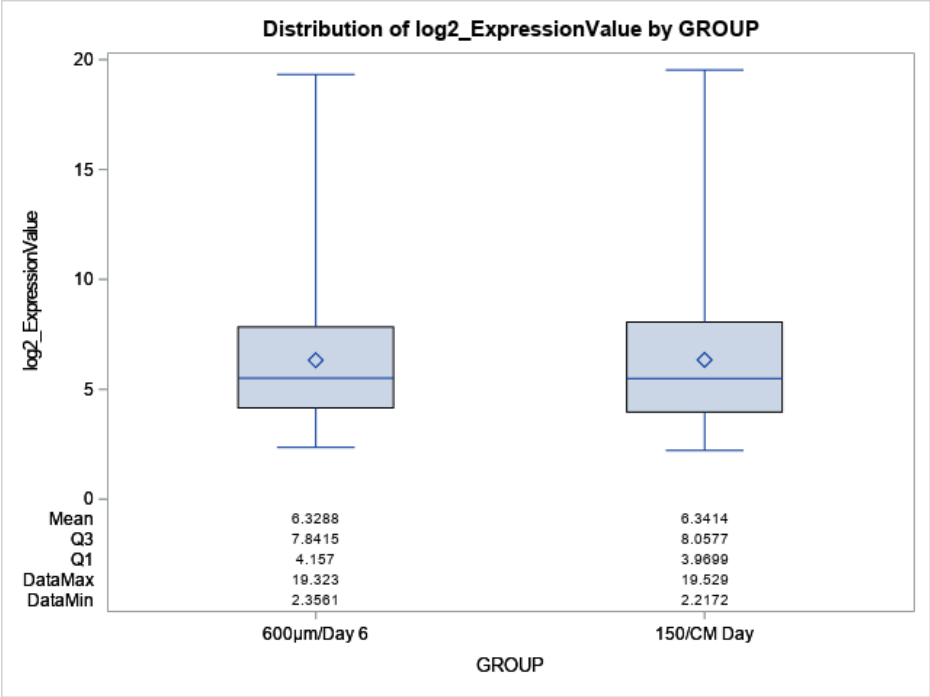

Figure 20: Boxplot of Log-2 transformed mean expression values of 600µm/Day 6 and 150/CM Day 6

Figure 20 represents the box plot generated from BOXPLOT function. Since the mean and upper quartile (75th percentile or Q3) of both groups is nearly the same, 6.3 is taken as the cutoff of Log-2 transformed mean expression values of both groups. Genes with Log-2 transformed mean expression values greater than 6.3 were filtered.

The filtered genes of both the datasets were compared and new lists with uncommon genes was created. To obtain the genes affecting migration function specifically, those lists where individually compared to migration related genes obtained from IPA Knowledgebase as shown in **Figure 21**.

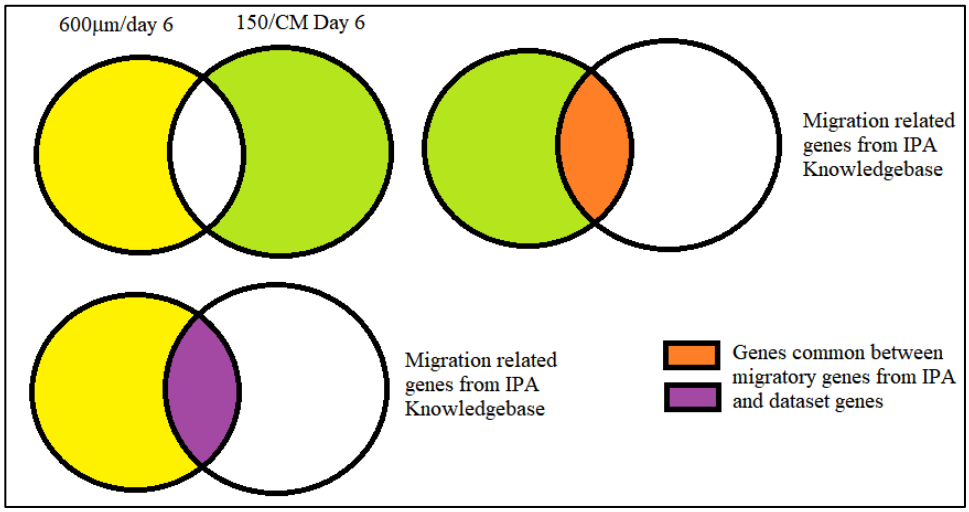

Figure 21: Pictorial representation of method used to obtain genes uncommon between 600µm/Day 6 and 150/CM Day 6 groups and affecting migration function

The genes obtained were inserted into My Pathway and were grown to connect to 'Migration of cells' function followed by overlaying all the canonical pathways (CP) containing migration of cells function and the dataset genes. Genes with no information of canonical pathway affecting migration function were trimmed.

Figure 22 and **23** show the network of genes from the 150/CM Day 6 and 600μm/Day 6 groups respectively and the 'migration of cells' function including the canonical pathways through which the interaction between genes and function occurs.

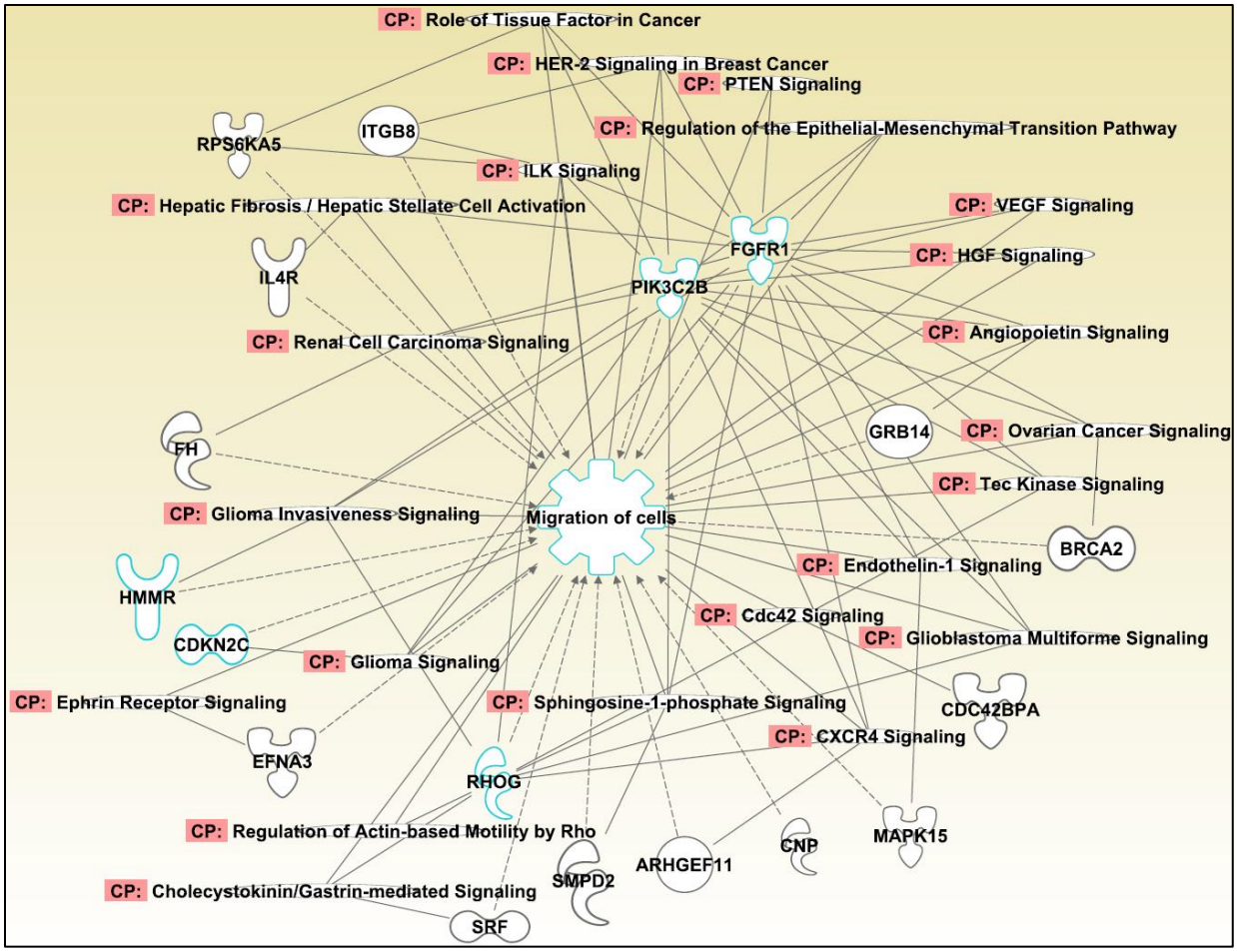

Figure 22: Network of genes from the 150/CM Day 6 group and the 'migration of cells' function including the canonical pathways through which the interaction between genes and function occurs

Figure 22 shows *EFNA3* (Ephrin A3), *SMPD2* (sphingomyelin phosphodiesterase 2), *SRF* (serum response factor), *CNP* (2',3'-cyclic nucleotide 3' phosphodiesterase), *MAPK15* (mitogen-activated protein kinase 15), *RHOG* (Ras homology growth-related), *CDC42BPA* (CDC42 binding protein kinase alpha), *CDKN2C* (cyclin dependent kinase inhibitor 2C), *HMMR* (hyaluronan mediated motility receptor), *BRCA2* (breast cancer genes 2), *PIK3C2B* (phosphatidylinositol-4-phosphate 3-kinase catalytic subunit type 2 beta), *FGFR1* (fibroblast growth factor receptor 1), *IL4R* (interleukin 4 receptor), *RPS6KA5* (ribosomal protein s6 kinase A5), *ITGB8* (integrin subunit beta 8), *GRB14* (growth factor receptor bound protein 14), *ARHGEF11* (rho guanine nucleotide

exchange factor 11), and *FH* (fumarate hydratase) genes that affect migration of cells function via different pathways.

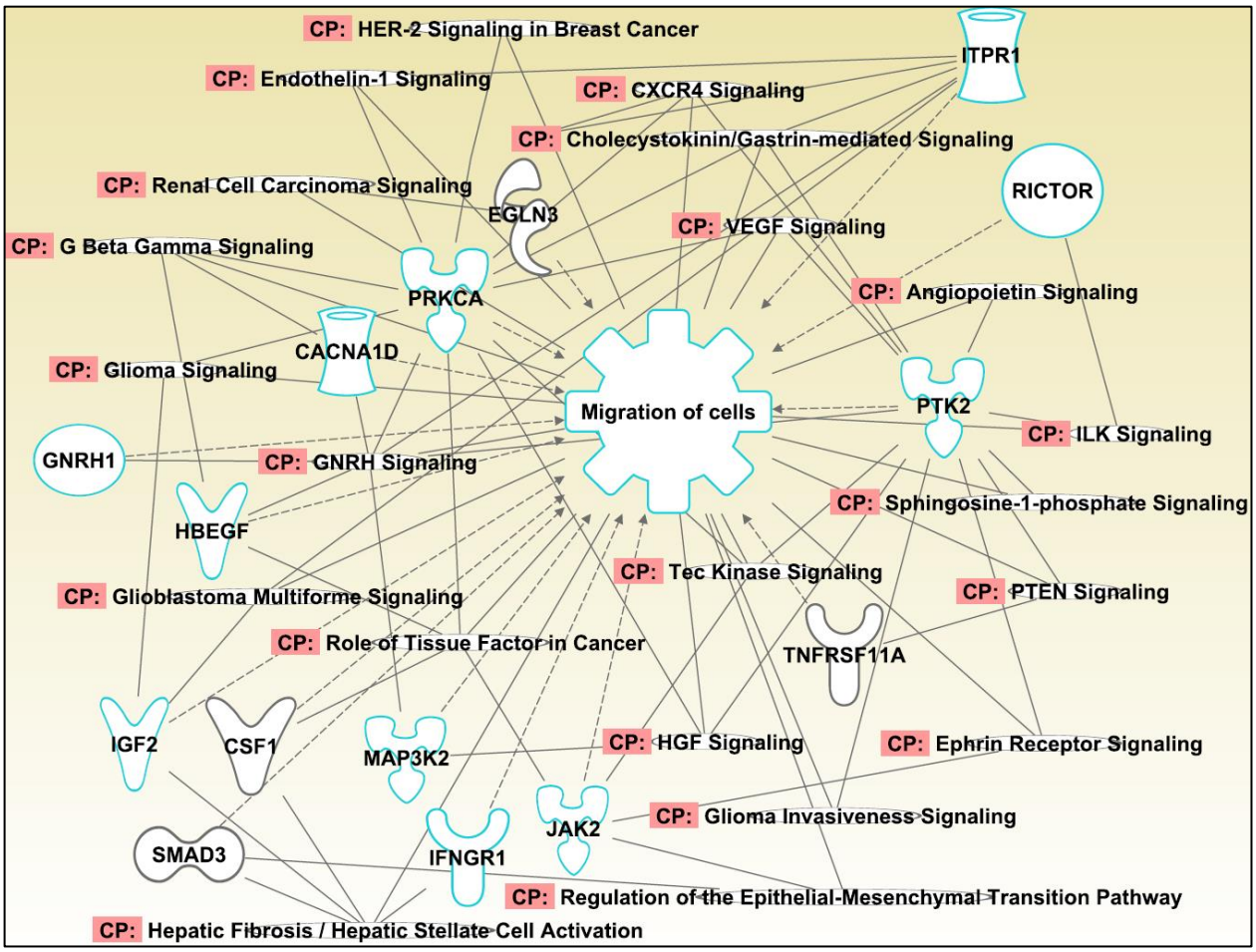

Figure 23: Network of genes from the 600µm/Day 6 group and the 'migration of cells' function including the canonical pathways through which the interaction between genes and function occurs

Figure 23 shows *GNRH1*, *HBEGF*, *IGF2* (insulin like growth factor 2), *CSF1* (colony stimulating factor 1), *MAP3K2* (mitogen-Activated Protein Kinase Kinase Kinase 2), *IFNGR1* (interferon gamma receptor 1), *SMAD3* (SMAD family member 3), *JAK2* (Janus kinase 2), *CACNA1D* (calcium voltage-gated channel subunit alpha1 D), *PRKCA* (protein kinase C Alpha), *PTK2* (protein tyrosine kinase 2), *TNFRSF11A* (TNF receptor superfamily member 11a), *EGLN3* (egl-9

family hypoxia inducible factor 3), and *RICTOR* (RPTOR independent companion of MTOR complex 2) genes that affect migration of cells function via different pathways. Out of these genes, *GNRH1, HBEGF, IGF2,* and *CSF1* genes are extracellular where *GNRH1, HBEGF* extracellular genes were also found in Figure 19 for 600µm/Day 6 *vs*. 150µm/Day 6 group.

Hence, the genes listed in Figure 22 and 23 might be the reason behind different migratory patterns of 600µm/Day 6 (tumor migrates in one direction) and 150µm/Day 6 (cells migrate in all directions) groups.

4 CONCLUSIONS AND FUTURE DIRECTIONS

Breast cancer is the second most common cause of cancer deaths in women. Breast cancer transitions from ductal hyperplasia (DH), and atypical ductal hyperplasia (ADH) (pre-malignant stages) to ductal carcinoma in situ (DCIS) (non-invasive) and invasive ductal carcinoma (IDC) (invasive stage) (malignant stage). Due to reported genomic level similarity in DCIS and IDC stage, there is a possibility of tumor microenvironment playing active role in DCIS to IDC transition. There are three hallmarks of DCIS to IDC transition, viz., increasing tumor size drives hypoxia and metabolic stress; heterogeneous tumor cells spontaneously emerge; and peripheral cells begin to migrate from the parent tumor.

Despite advancements in the diagnostic procedures used in breast cancer, many challenges remain to be addressed such as treatment of local recurrence and metastasis; ability to predict the risk of progression from pre-invasive to invasive disease; and overtreatment of patients that are not at risk. To overcome these challenges, it is crucial to study the markers inducing pre-invasive to invasive transition. There is a lack of experimental models with controlled tumor microenvironments to capture DCIS to IDC transition. Therefore, it is desirable to have a high throughput 3-D experimental system that recapitulates a spontaneously formed hypoxic tumor microenvironment without interference from other non-cancerous cells. To overcome the limitations of current models, our lab has developed uniform-sized, 3-D *in vitro* microtumors with controlled microenvironment using PEGDMA hydrogel microwells. Without any external stimulus, the precise control over the size of these microtumors exhibits three key hallmarks of pre-invasive to invasive disease transition observed *in vivo*. We have developed three controlled model systems: 1) non-hypoxic, non-migratory small microtumors (150μm/Day 6); 2) hypoxic,

migratory large microtumors (600μm/Day 6); and 3) non-hypoxic, yet migratory small microtumors treated with tumor-secreted factors (secretome) using the conditioned media (CM) of large microtumors (150/CM Day 6). The objective of this study is to delineate the role of microtumor size (hypoxic microenvironment), time and tumor-secreted factors (conditioned media) in inducing migratory phenotypes in non-migratory parental cells. To understand the mechanisms of spontaneous emergence of migratory phenotypes in large hypoxic migratory microtumors (600μm/Day 6) and small non-hypoxic yet migratory microtumors (150/CM Day 6), we performed quantitative analysis of RNA expression using Affymetrix gene chip cDNA microarrays. We utilized non-hypoxic small microtumors (150μm/Day 6) and early stage large microtumors (600μm/Day 1) as controls of non-migratory phenotypes. The raw data were analyzed using Transcriptome Analysis Console (TAC) and Ingenuity Pathway Analysis (IPA).

Analysis of 600μm/Day 6 *vs*. 600μm/Day 1 indicates the temporal effect, which caused downregulation in the cholesterol biosynthesis pathways, and interferon signaling pathways. On the other hand, upregulation was observed in the cell cycle checkpoint regulation pathways, ATM signaling and sirtuin signaling pathway. This indicated that stress-induced pathways were activated due to temporal effect. From the canonical pathways, prevalence of hypoxic conditions in large tumors was deduced. *MB*, *COMT*, *DLL4*, and *PARK7* genes were found to regulate hypoxic conditions which in turn affected *VEGFA*, *GNA12*, *CA12*, and *CA9* genes via multiple pathways. *RARB*, and *BRD4* were the upstream regulators that were responsible for the observed gene expression affecting 'migration of cells' function. *PCSK6*, *LCN2*, *AGT*, *CSF1*, *VEGF*, *ECM1*, *CCL20*, *NDNF*, *MTUS1* were the extracellular genes that induced migration of cells function. Similarly, to test the effect of size of microtumors on migration of cells, analysis of 600μm/Day 6 *vs*. 150μm/Day 6 was performed which indicated downregulation of cholesterol biosynthesis

pathways but upregulation of cell cycle checkpoint regulation pathways, ATM signaling and sirtuin signaling pathways. Hence, stress-induced pathways were activated due to size-effect (hypoxic microenvironments), which implies that we successfully developed microtumor models with hypoxic and non-hypoxic microenvironment by engineering tumor size. *CA12, CA9, COMT, DLL4, GNAI2, MB, PARK7, VEGFA* genes were shown to be related to hypoxic function and *LGALS3, LOX, ADM, VEGF, HBEGF, CXCL9, AREG, LCN2, BMP4, TNFSF10, GAST, DLL4, ECM1, STC1, TGFB1* were the upregulated extracellular molecules that affected migration of cells function. *COL18A1,* and *ER* were the upstream regulators that influence dataset genes affecting migration of genes.

To test the role of secreted factors from large migratory tumors on the migration of small non-migratory tumors, 150 µm tumors were subjected to 600 µm tumor-conditioned media for 3 days. Normalizing this 150/CM Day 6 (150 µm tumors subjected to large microtumor media) group with 150 µm/Day 6 gave us the secretome effect as both the microtumors were of the same size (150 µm) and were harvested on the same day. Unlike 600µm/Day 6 *vs.* 150µm/Day 6 and 600µm/Day 6 *vs.* 600µm/Day 1 groups, comparison between 150/CM Day 6 and 150µm/Day 6 microtumor models revealed no significant effect on the cholesterol biosynthesis pathways. p53 and ATM signaling pathways were downregulated in 150/CM Day 6 *vs.* 150µm/Day 6 microtumor models in contrast to their upregulation in 600µm/Day 6 *vs.* 150µm/Day 6 and 600µm/Day 6 *vs.* 600µm/Day 1. Regulation of actin-based motility by Rho pathway and interferon signaling pathways were significantly upregulated in 150/CM Day 6 *vs.* 150µm/Day 6. Stress-induced pathways were inhibited, and migration-inducing pathways were activated due to secretome effect. This showed that secretome of hypoxic microtumors did not induce any stress related pathways.

Differences in the migratory pattern between 600μm/Day 6 and 150/CM Day 6 were observed where large hypoxic (600μm) microtumors exhibited directionality while migrating, whereas secretome-induced migration in 150/CM did not show any directionality. We hypothesized that such differences could be attributed to the differences in gene expression and thus, mechanisms driving the migratory phenotype. Network diagram was constructed from genes uncommon between 150/CM Day 6 and 600μm/Day 6 affecting the migration function. Canonical pathways constituting the dataset genes affecting migration function were overlaid. This resulted in *EFNA3, SMPD2, SRF, CNP, MAPK15, RHOG, CDC42BPA, CDKN2C, HMMR, BRCA2, PIK3C2B, FGFR1, IL4R, RPS6KA5, ITGB8, GRB14, ARHGEF11,* and *FH* genes from 150/CM Day 6 group and *GNRH1, HBEGF, IGF2, CSF1, MAP3K2, IFNGR1, SMAD3, JAK2, CACNA1D, PRKCA, PTK2, TNFRSF11A, EGLN3,* and *RICTOR* genes from 600μm/Day 6 that affect migration of cells function via different pathways.

Thus, by studying the differential gene expression of migratory groups *vs.* non-migratory groups, we identify genes that are differentially expressed in pre-invasive and invasive stages of breast cancer as migration is one of the hallmarks of DCIS to IDC transition. Also, by further investigating the effect of size of microtumor, time for growth of microtumors and secreted factors from migrating microtumors on migration of non-migratory tumor, we can understand how these different factors selectively contribute to emergence of the migratory phenotype using *in vitro* 3-D microtumor models with controlled microenvironment.

Future Studies:

To further validate the prevalence of hypoxia in 600μm/Day 6 and absence in 150/CM Day 6, oxygen consumption rate (OCR) and extracellular acidification rate (ECAR) of live cells in 600μm/Day 6 and 150/CM Day 6 need to be tested using Seahorse XF Analyzers. Genes affecting

hypoxia emerged due to temporal and size effect need to be validated using qRT-PCR. Similar pathway and functional analysis can be performed on MetaCore software to correlate the results produced from IPA and MetaCore software. Secretome studies of each group will further help validate the extracellular molecules and surface proteome (plasma membrane receptors) expressed in migratory tumors in comparison with non-migratory tumors.

5 ABBREVIATIONS

DH	Ductal hyperplasia
ADH	Atypical ductal hyperplasia
DCIS	Ductal carcinoma *in situ*
IDC	Invasive ductal carcinoma
HER2/NEU	Human epidermal growth factor receptor 2
ER	Estrogen receptor
PR	Progesterone receptor
ECM	Extracellular matrix
TME	Tumor microenvironment
HIF-1	Hypoxia-inducible factor 1
MMP	Matrix metalloproteases
SIM2s S	Single-minded
FOXC2	Forkhead box protein C2
SNAIL	Zinc finger protein SNAI1
ZEB1	Zinc finger E-box binding homeobox 1
ZEB2	Zinc finger E-box binding homeobox 2
2-D	Two-dimensional T
3-D	Three-dimensional
HMF	Human mammary fibroblast
PDMS	Polydimethylsiloxane
PEGDMA	Polyethylene glycol dimethacrylate
E-CAD	E-Cadherin

VIM	Vimentin
RNA-seq	RNA sequencing
lncRNAs	Long non-coding RNAs
LCM	Laser capture microdissecion
cDNA	Complementary DNA
RT-qPCR	Real-time quantitative polymerase chain reaction
FEPE	Fixed formalin paraffin
TAC	Transcriptome analysis console
IPA	Ingenuity Pathway Analysis
URA	Upstream regulator analysis
MN	Mechanistic networks
CAN	Causal Network analysis
DEA	Downstream effect analysis
FDR	False discovery rate
FC	Fold change
MAP	Molecular activity predictor
CA5B	Carbonic anhydrase 5B
CA9	Carbonic anhydrase IX
NR3C1	Nuclear receptor subfamily 3 group c member 1
SLC7A11	Solute carrier family 7 member 11
PDE8A	Phosphodiesterase 8A
MB	Myoglobin
TMEM38B	Transmembrane protein 38B

PARK7	Parkinsonism associated deglycase
RARB	Retinoic acid receptor beta
BRD4	Bromodomain-containing protein 4
CP	Canonical pathways
PCSK6	Proprotein convertase subtilisin/kexin type 6
LCN2	Lipocalin 2
AGT	Angiotensinogen
CSF1	Colony stimulating factor 1
VEGF	Vascular endothelial growth factor
ECM1	Extracellular matrix protein 1
CCL20	Chemokine (c-c motif) ligand 20
CA12	Carbonic anhydrase 12
COMT	Catechol-O-methyltransferase
DLL4	Delta-like protein 4
PARK7	Parkinsonism associated deglycase
COL18A1	Collagen type XVIII alpha 1 chain
ER	Estrogen receptor
LGALS3	Galectin 3
LOX	Lysyl oxidase
ADM	Adrenomedullin
HBEGF	Heparin-binding egf-like growth factor
CXCL9	Chemokine (c-x-c motif) ligand 9
AREG	Amphiregulin

BMP4	Bone morphogenetic protein 4
TNFSF10	Tumor necrosis factor (ligand) superfamily, member 10
GAST	Gastrin
STC1	Stanniocalcin-1
TGFB1	Transforming growth factor beta 1
EFNA3	Ephrin A3
SMPD2	Sphingomyelin phosphodiesterase 2
SRF	Serum response factor
CNP	2',3'-cyclic nucleotide 3' phosphodiesterase
MAPK15	Mitogen-activated protein kinase 15
RHOG	Ras homology growth-related
CDC42BPA	CDC42 binding protein kinase alpha
CDKN2C	Cyclin dependent kinase inhibitor 2C
HMMR	Hyaluronan mediated motility receptor
BRCA2	Breast cancer genes 2
PIK3C2B	Phosphatidylinositol-4-phosphate 3-kinase catalytic subunit type 2 beta
FGFR1	Fibroblast growth factor receptor 1
IL4R	Interleukin 4 receptor
RPS6KA5	Ribosomal protein s6 kinase A5
ITGB8	Integrin subunit beta 8
GRB14	Growth factor receptor bound protein 14
ARHGEF11	Rho guanine nucleotide exchange factor 11
FH	Fumarate hydratase

IGF2	Insulin like growth factor 2
CSF1	Colony stimulating factor 1
MAP3K2	Mitogen-Activated Protein Kinase Kinase Kinase 2
IFNGR1	Interferon gamma receptor 1
SMAD3	SMAD family member 3
JAK2	Janus kinase 2
CACNA1D	Calcium voltage-gated channel subunit alpha1 D
PRKCA	Protein kinase C Alpha
PTK2	Protein tyrosine kinase 2
TNFRSF11A	TNF receptor superfamily member 11a
EGLN3	Egl-9 family hypoxia inducible factor 3
RICTOR	RPTOR independent companion of MTOR complex 2

BIBLIOGRAPHY

1. Centers for disease control and prevention. What is breast cancer? **2018** https://www.cdc.gov/cancer/breast/basic_info/what-is-breast-cancer.htm.

2. Mayo clinic, Breast cancer. **2019**.

3. American cancer society. *Cancer facts and figures 2019*; 2019.

4. Mayo Clinic. Breast anatomy, https://www.mayoclinic.org/breast-anatomy/img-20007078.

5. MedicineNet. Breast Anatomy. https://www.medicinenet.com/breast_anatomy/article.htm#what_should_i_know_about_breast.

6. Bombonati, A.; Sgroi, D. C., The molecular pathology of breast cancer progression. *The Journal of pathology* **2011,** *223* (2), 307-317.

7. Casasent, A. K.; Edgerton, M.; Navin, N. E., Genome evolution in ductal carcinoma in situ: invasion of the clones. *J Pathol* **2017,** *241* (2), 208-218.

8. National breast cancer foundation, i. Invasive Ductal Carcinoma. https://www.nationalbreastcancer.org/invasive-ductal-carcinoma.

9. Ernster, V. L.; Barclay, J., Increases in ductal carcinoma in situ (DCIS) of the breast in relation to mammography: a dilemma. *J Natl Cancer Inst Monogr* **1997,** (22), 151-6.

10. Baxter, N. N.; Virnig, B. A.; Durham, S. B.; Tuttle, T. M., Trends in the treatment of ductal carcinoma in situ of the breast. *J Natl Cancer Inst* **2004,** *96* (6), 443-8.

11. Zujewski, J. A.; Harlan, L. C.; Morrell, D. M.; Stevens, J. L., Ductal carcinoma in situ: trends in treatment over time in the US. *Breast Cancer Res Treat* **2011,** *127* (1), 251-7.

12. Jones, J. L., Overdiagnosis and overtreatment of breast cancer: progression of ductal carcinoma in situ: the pathological perspective. *Breast Cancer Res* **2006,** *8* (2), 204.

13. Mastectomy or lumpectomy? The choice of operation for clinical stages I and II breast cancer. The Steering Committee on Clinical Practice Guidelines for the Care and Treatment of Breast Cancer. Canadian Association of Radiation Oncologists. *CMAJ : Canadian Medical Association journal = journal de l'Association medicale canadienne* **1998,** *158 Suppl 3*, S15-21.

14. Shah, R.; Rosso, K.; Nathanson, S. D., Pathogenesis, prevention, diagnosis and treatment of breast cancer. *World journal of clinical oncology* **2014,** *5* (3), 283-298.

15. Pace, L. E.; Keating, N. L., A Systematic Assessment of Benefits and Risks to Guide Breast Cancer Screening DecisionsBreast Cancer Screening DecisionsBreast Cancer Screening Decisions. *JAMA* **2014,** *311* (13), 1327-1335.

16. McDonald, E. S.; Clark, A. S.; Tchou, J.; Zhang, P.; Freedman, G. M., Clinical Diagnosis and Management of Breast Cancer. *Journal of nuclear medicine : official publication, Society of Nuclear Medicine* **2016,** *57 Suppl 1*, 9s-16s.

17. Yamaguchi, H.; Wyckoff, J.; Condeelis, J., Cell migration in tumors. *Current opinion in cell biology* **2005,** *17* (5), 559-64.

18. Khalil, A. A.; Ilina, O.; Gritsenko, P. G.; Bult, P.; Span, P. N.; Friedl, P., Collective invasion in ductal and lobular breast cancer associates with distant metastasis. *Clinical & Experimental Metastasis* **2017,** *34* (6), 421-429.

19. Soysal, S. D.; Tzankov, A.; Muenst, S. E., Role of the Tumor Microenvironment in Breast Cancer. *Pathobiology* **2015,** *82* (3-4), 142-152.

20. Petridis, C.; Brook, M. N.; Shah, V.; Kohut, K.; Gorman, P.; Caneppele, M.; Levi, D.; Papouli, E.; Orr, N.; Cox, A.; Cross, S. S.; dos-Santos-Silva, I.; Peto, J.; Swerdlow, A.;

Schoemaker, M. J.; Bolla, M. K.; Wang, Q.; Dennis, J.; Michailidou, K.; Benitez, J.; González-Neira, A.; Tessier, D. C.; Vincent, D.; Li, J.; Figueroa, J.; Kristensen, V.; Borresen-Dale, A.-L.; Soucy, P.; Simard, J.; Milne, R. L.; Giles, G. G.; Margolin, S.; Lindblom, A.; Brüning, T.; Brauch, H.; Southey, M. C.; Hopper, J. L.; Dörk, T.; Bogdanova, N. V.; Kabisch, M.; Hamann, U.; Schmutzler, R. K.; Meindl, A.; Brenner, H.; Arndt, V.; Winqvist, R.; Pylkäs, K.; Fasching, P. A.; Beckmann, M. W.; Lubinski, J.; Jakubowska, A.; Mulligan, A. M.; Andrulis, I. L.; Tollenaar, R. A. E. M.; Devilee, P.; Le Marchand, L.; Haiman, C. A.; Mannermaa, A.; Kosma, V.-M.; Radice, P.; Peterlongo, P.; Marme, F.; Burwinkel, B.; van Deurzen, C. H. M.; Hollestelle, A.; Miller, N.; Kerin, M. J.; Lambrechts, D.; Floris, G.; Wesseling, J.; Flyger, H.; Bojesen, S. E.; Yao, S.; Ambrosone, C. B.; Chenevix-Trench, G.; Truong, T.; Guénel, P.; Rudolph, A.; Chang-Claude, J.; Nevanlinna, H.; Blomqvist, C.; Czene, K.; Brand, J. S.; Olson, J. E.; Couch, F. J.; Dunning, A. M.; Hall, P.; Easton, D. F.; Pharoah, P. D. P.; Pinder, S. E.; Schmidt, M. K.; Tomlinson, I.; Roylance, R.; García-Closas, M.; Sawyer, E. J., Genetic predisposition to ductal carcinoma in situ of the breast. *Breast Cancer Research* **2016,** *18* (1), 22.

21. Sopik, V.; Narod, S. A., Common genetic susceptibility to DCIS and invasive ductal carcinoma. *Breast Cancer Research* **2016,** *18* (1), 60.

22. Newman, S.; Howarth, K. D.; Greenman, C. D.; Bignell, G. R.; Tavaré, S.; Edwards, P. A. W., The Relative Timing of Mutations in a Breast Cancer Genome. *PLOS ONE* **2013,** *8* (6), e64991.

23. Lo, P. K.; Zhang, Y.; Yao, Y.; Wolfson, B.; Yu, J.; Han, S. Y.; Duru, N.; Zhou, Q., Tumor-associated myoepithelial cells promote the invasive progression of ductal carcinoma in situ through activation of TGFbeta signaling. *J Biol Chem* **2017,** *292* (27), 11466-11484.

24. Espina, V.; Mariani, B. D.; Gallagher, R. I.; Tran, K.; Banks, S.; Wiedemann, J.; Huryk, H.; Mueller, C.; Adamo, L.; Deng, J.; Petricoin, E. F.; Pastore, L.; Zaman, S.; Menezes, G.; Mize, J.; Johal, J.; Edmiston, K.; Liotta, L. A., Malignant precursor cells pre-exist in human breast DCIS and require autophagy for survival. *PLoS One* **2010,** *5* (4), e10240.

25. Ma, X.-J.; Dahiya, S.; Richardson, E.; Erlander, M.; Sgroi, D. C., Gene expression profiling of the tumor microenvironment during breast cancer progression. *Breast Cancer Research* **2009,** *11* (1), R7.

26. Ma, X.-J.; Salunga, R.; Tuggle, J. T.; Gaudet, J.; Enright, E.; McQuary, P.; Payette, T.; Pistone, M.; Stecker, K.; Zhang, B. M.; Zhou, Y.-X.; Varnholt, H.; Smith, B.; Gadd, M.; Chatfield, E.; Kessler, J.; Baer, T. M.; Erlander, M. G.; Sgroi, D. C., Gene expression profiles of human breast cancer progression. *Proceedings of the National Academy of Sciences* **2003,** *100* (10), 5974-5979.

27. Place, A. E.; Jin Huh, S.; Polyak, K., The microenvironment in breast cancer progression: biology and implications for treatment. *Breast Cancer Res* **2011,** *13* (6), 227.

28. Cowell, C. F.; Weigelt, B.; Sakr, R. A.; Ng, C. K. Y.; Hicks, J.; King, T. A.; Reis-Filho, J. S., Progression from ductal carcinoma in situ to invasive breast cancer: revisited. *Molecular oncology* **2013,** *7* (5), 859-869.

29. Hoarau-Véchot, J.; Rafii, A.; Touboul, C.; Pasquier, J., Halfway between 2D and Animal Models: Are 3D Cultures the Ideal Tool to Study Cancer-Microenvironment Interactions? *International journal of molecular sciences* **2018,** *19* (1), 181.

30. Singh, M.; Venkata Krishnan, H.; Ranganathan, S.; Kiesel, B.; Beumer, J. H.; Sreekumar, S.; Sant, S., Controlled Three-Dimensional Tumor Microenvironments Recapitulate Phenotypic

Features and Differential Drug Response in Early vs Advanced Stage Breast Cancer. *ACS Biomaterials Science & Engineering* **2018,** *4* (2), 421-431.

31. Wang, M.; Zhao, J.; Zhang, L.; Wei, F.; Lian, Y.; Wu, Y.; Gong, Z.; Zhang, S.; Zhou, J.; Cao, K.; Li, X.; Xiong, W.; Li, G.; Zeng, Z.; Guo, C., Role of tumor microenvironment in tumorigenesis. *Journal of Cancer* **2017,** *8* (5), 761-773.

32. Balkwill, F. R.; Capasso, M.; Hagemann, T., The tumor microenvironment at a glance. *Journal of Cell Science* **2012,** *125* (23), 5591-5596.

33. Rankin, E. B.; Nam, J.-M.; Giaccia, A. J., Hypoxia: Signaling the Metastatic Cascade. *Trends in Cancer* **2016,** *2* (6), 295-304.

34. Vaupel, P.; Mayer, A.; Hockel, M., Tumor hypoxia and malignant progression. *Methods Enzymol* **2004,** *381*, 335-54.

35. Hockel, M.; Schlenger, K.; Aral, B.; Mitze, M.; Schaffer, U.; Vaupel, P., Association between tumor hypoxia and malignant progression in advanced cancer of the uterine cervix. *Cancer Res* **1996,** *56* (19), 4509-15.

36. Hockel, M.; Schlenger, K.; Hockel, S.; Aral, B.; Schaffer, U.; Vaupel, P., Tumor hypoxia in pelvic recurrences of cervical cancer. *Int J Cancer* **1998,** *79* (4), 365-9.

37. Semenza, G. L., Defining the role of hypoxia-inducible factor 1 in cancer biology and therapeutics. *Oncogene* **2010,** *29* (5), 625-34.

38. Wong, C. C.-L.; Gilkes, D. M.; Zhang, H.; Chen, J.; Wei, H.; Chaturvedi, P.; Fraley, S. I.; Wong, C.-M.; Khoo, U.-S.; Ng, I. O.-L.; Wirtz, D.; Semenza, G. L., Hypoxia-inducible factor 1 is a master regulator of breast cancer metastatic niche formation. *Proceedings of the National Academy of Sciences* **2011,** *108* (39), 16369-16374.

39. Reid, M. A.; Kong, M., Dealing with hunger: Metabolic stress responses in tumors. *Journal of carcinogenesis* **2013,** *12*, 17-17.

40. Jones, R. G.; Thompson, C. B., Tumor suppressors and cell metabolism: a recipe for cancer growth. *Genes & development* **2009,** *23* (5), 537-48.

41. Patel, S.; Ngounou Wetie, A. G.; Darie, C. C.; Clarkson, B. D., Cancer secretomes and their place in supplementing other hallmarks of cancer. *Adv Exp Med Biol* **2014,** *806*, 409-42.

42. Place, A. E.; Jin Huh, S.; Polyak, K., The microenvironment in breast cancer progression: biology and implications for treatment. *Breast cancer research : BCR* **2011,** *13* (6), 227-227.

43. Hu, M.; Yao, J.; Carroll, D. K.; Weremowicz, S.; Chen, H.; Carrasco, D.; Richardson, A.; Violette, S.; Nikolskaya, T.; Nikolsky, Y.; Bauerlein, E. L.; Hahn, W. C.; Gelman, R. S.; Allred, C.; Bissell, M. J.; Schnitt, S.; Polyak, K., Regulation of in situ to invasive breast carcinoma transition. *Cancer cell* **2008,** *13* (5), 394-406.

44. Nicolson, G. L., Generation of phenotypic diversity and progression in metastatic tumor cells. *Cancer metastasis reviews* **1984,** *3* (1), 25-42.

45. Scribner, K. C.; Behbod, F.; Porter, W. W., Regulation of DCIS to invasive breast cancer progression by Singleminded-2s (SIM2s). *Oncogene* **2013,** *32* (21), 2631-9.

46. Mueller, K. L.; Madden, J. M.; Zoratti, G. L.; Kuperwasser, C.; List, K.; Boerner, J. L., Fibroblast-secreted hepatocyte growth factor mediates epidermal growth factor receptor tyrosine kinase inhibitor resistance in triple-negative breast cancers through paracrine activation of Met. *Breast Cancer Research* **2012,** *14* (4), R104.

47. Li, Q.; Xia, J.; Yao, Y.; Gong, D.-W.; Shi, H.; Zhou, Q., Sulforaphane inhibits mammary adipogenesis by targeting adipose mesenchymal stem cells. *Breast cancer research and treatment* **2013,** *141* (2), 317-324.

48. Duval, K.; Grover, H.; Han, L.-H.; Mou, Y.; Pegoraro, A. F.; Fredberg, J.; Chen, Z., Modeling Physiological Events in 2D vs. 3D Cell Culture. *Physiology (Bethesda, Md.)* **2017,** *32* (4), 266-277.

49. Espina, V.; Wysolmerski, J.; Edmiston, K.; Liotta, L. A., Attacking breast cancer at the preinvasion stage by targeting autophagy. *Women's health (London, England)* **2013,** *9* (2), 157-170.

50. Helczynska, K.; Kronblad, Å.; Jögi, A.; Nilsson, E.; Beckman, S.; Landberg, G.; Påhlman, S., Hypoxia Promotes a Dedifferentiated Phenotype in Ductal Breast Carcinoma *in situ*. *Cancer Research* **2003,** *63* (7), 1441-1444.

51. Sant, S.; Johnston, P. A., The production of 3D tumor spheroids for cancer drug discovery. *Drug Discov Today Technol* **2017,** *23*, 27-36.

52. Carter, E. P.; Gopsill, J. A.; Gomm, J. J.; Jones, J. L.; Grose, R. P., A 3D in vitro model of the human breast duct: a method to unravel myoepithelial-luminal interactions in the progression of breast cancer. *Breast Cancer Research* **2017,** *19* (1), 50.

53. Osuala, K. O.; Sameni, M.; Shah, S.; Aggarwal, N.; Simonait, M. L.; Franco, O. E.; Hong, Y.; Hayward, S. W.; Behbod, F.; Mattingly, R. R.; Sloane, B. F., Il-6 signaling between ductal carcinoma in situ cells and carcinoma-associated fibroblasts mediates tumor cell growth and migration. *BMC Cancer* **2015,** *15* (1), 584.

54. Bischel, L. L.; Beebe, D. J.; Sung, K. E., Microfluidic model of ductal carcinoma in situ with 3D, organotypic structure. *BMC cancer* **2015,** *15*, 12-12.

55. Wang, Y.; Mirza, S.; Wu, S.; Zeng, J.; Shi, W.; Band, H.; Band, V.; Duan, B., 3D hydrogel breast cancer models for studying the effects of hypoxia on epithelial to mesenchymal transition. *Oncotarget* **2018,** *9* (63), 32191-32203.

56. Menon, J., *3D tumor models for cancer drug discovery: Current status and outlook*. 2018; Vol. 2, p 1-2.

57. George, A. L.; Rajoria, S.; Suriano, R.; Mittleman, A.; Tiwari, R. K., Hypoxia and estrogen are functionally equivalent in breast cancer-endothelial cell interdependence. *Molecular cancer* **2012,** *11*, 80.

58. Vaapil, M.; Helczynska, K.; Villadsen, R.; Petersen, O. W.; Johansson, E.; Beckman, S.; Larsson, C.; Påhlman, S.; Jögi, A., Hypoxic Conditions Induce a Cancer-Like Phenotype in Human Breast Epithelial Cells. *PLOS ONE* **2012,** *7* (9), e46543.

59. Singh, M.; Tian, X.-J.; Donnenberg, V. S.; Watson, A. M.; Zhang, J.; Stabile, L. P.; Watkins, S. C.; Xing, J.; Sant, S., Targeting temporal dynamics of microenvironmental factors halts tumor migration and alleviates effects of dynamic tumor heterogeneity. *bioRxiv* **2017**, 191221.

60. Singh, M.; Mukundan, S.; Jaramillo, M.; Oesterreich, S.; Sant, S., Three-Dimensional Breast Cancer Models Mimic Hallmarks of Size-Induced Tumor Progression. *Cancer Res* **2016,** *76* (13), 3732-43.

61. Singh, M.; Close, D. A.; Mukundan, S.; Johnston, P. A.; Sant, S., Production of Uniform 3D Microtumors in Hydrogel Microwell Arrays for Measurement of Viability, Morphology, and Signaling Pathway Activation. *Assay Drug Dev Technol* **2015,** *13* (9), 570-83.

62. Singh, M.; Warita, K.; Warita, T.; Faeder, J.; Lee, R.; Sant, S.; N. Oltvai, Z., *Shift from stochastic to spatially-ordered expression of serine-glycine synthesis enzymes in 3D microtumors*. 2018; Vol. 8.

63. Xu, Y.; Qin, L.; Sun, T.; Wu, H.; He, T.; Yang, Z.; Mo, Q.; Liao, L.; Xu, J., Twist1 promotes breast cancer invasion and metastasis by silencing Foxa1 expression. *Oncogene* **2017,** *36* (8), 1157-1166.

64. Banin Hirata, B. K.; Oda, J. M. M.; Losi Guembarovski, R.; Ariza, C. B.; Oliveira, C. E. C. d.; Watanabe, M. A. E., Molecular Markers for Breast Cancer: Prediction on Tumor Behavior. *Disease Markers* **2014,** *2014*, 12.

65. Lin, H. Y.; Sun, S. M.; Lu, X. F.; Chen, P. Y.; Chen, C. F.; Liang, W. Q.; Peng, C. Y., CCR10 activation stimulates the invasion and migration of breast cancer cells through the ERK1/2/MMP-7 signaling pathway. *International immunopharmacology* **2017,** *51*, 124-130.

66. Wang, Z.; Gerstein, M.; Snyder, M., RNA-Seq: a revolutionary tool for transcriptomics. *Nature reviews. Genetics* **2009,** *10* (1), 57-63.

67. Tarca, A. L.; Romero, R.; Draghici, S., Analysis of microarray experiments of gene expression profiling. *American journal of obstetrics and gynecology* **2006,** *195* (2), 373-388.

68. Nazarov, P. V.; Muller, A.; Kaoma, T.; Nicot, N.; Maximo, C.; Birembaut, P.; Tran, N. L.; Dittmar, G.; Vallar, L., RNA sequencing and transcriptome arrays analyses show opposing results for alternative splicing in patient derived samples. *BMC genomics* **2017,** *18* (1), 443-443.

69. Kukurba, K. R.; Montgomery, S. B., RNA Sequencing and Analysis. *Cold Spring Harbor protocols* **2015,** *2015* (11), 951-969.

70. Bumgarner, R., Overview of DNA microarrays: types, applications, and their future. *Current protocols in molecular biology* **2013,** *Chapter 22*, Unit-22.1.

71. Wang, Z.; Gerstein, M.; Snyder, M., RNA-Seq: a revolutionary tool for transcriptomics. *Nature Reviews Genetics* **2009,** *10*, 57.

72. Lowe, R.; Shirley, N.; Bleackley, M.; Dolan, S.; Shafee, T., Transcriptomics technologies. *PLOS Computational Biology* **2017,** *13* (5), e1005457.

73. Subio inc Rna-seq vs. Microarray. https://www.subioplatform.com/products/subioplatform/rna-seq-vs-microarray.

74. Sgroi, D. C.; Teng, S.; Robinson, G.; LeVangie, R.; Hudson, J. R.; Elkahloun, A. G., In Vivo Gene Expression Profile Analysis of Human Breast Cancer Progression. *Cancer research* **1999,** *59* (22), 5656-5661.

75. Luzzi, V.; Holtschlag, V.; Watson, M. A., Expression Profiling of Ductal Carcinoma in Situ by Laser Capture Microdissection and High-Density Oligonucleotide Arrays. *The American Journal of Pathology* **2001,** *158* (6), 2005-2010.

76. Mak, I. W.; Evaniew, N.; Ghert, M., Lost in translation: animal models and clinical trials in cancer treatment. *American journal of translational research* **2014,** *6* (2), 114-8.

77. Geneticist. The pros and cons of ffpe vs frozen tissue samples. https://www.geneticistinc.com/blog/the-pros-and-cons-of-ffpe-vs-frozen-tissue-samples.

78. Kaur, G.; Dufour, J. M., Cell lines: Valuable tools or useless artifacts. *Spermatogenesis* **2012,** *2* (1), 1-5.

79. Geiger, T.; Madden, S. F.; Gallagher, W. M.; Cox, J.; Mann, M., Proteomic Portrait of Human Breast Cancer Progression Identifies Novel Prognostic Markers. *Cancer research* **2012,** *72* (9), 2428-2439.

80. Calaf, G. M.; Abarca-Quinones, J., Ras protein expression as a marker for breast cancer. *Oncology letters* **2016,** *11* (6), 3637-3642.

81. Maguire, S. L.; Peck, B.; Wai, P. T.; Campbell, J.; Barker, H.; Gulati, A.; Daley, F.; Vyse, S.; Huang, P.; Lord, C. J.; Farnie, G.; Brennan, K.; Natrajan, R., Three-dimensional

modelling identifies novel genetic dependencies associated with breast cancer progression in the isogenic MCF10 model. *The Journal of Pathology* **2016,** *240* (3), 315-328.

82. Krämer, A.; Green, J.; Pollard, J., Jr.; Tugendreich, S., Causal analysis approaches in Ingenuity Pathway Analysis. *Bioinformatics (Oxford, England)* **2014,** *30* (4), 523-530.

83. Rye, M. B.; Bertilsson, H.; Andersen, M. K.; Rise, K.; Bathen, T. F.; Drabløs, F.; Tessem, M.-B., Cholesterol synthesis pathway genes in prostate cancer are transcriptionally downregulated when tissue confounding is minimized. *BMC cancer* **2018,** *18* (1), 478-478.

84. Olcina, M. M.; Grand, R. J.; Hammond, E. M., ATM activation in hypoxia - causes and consequences. *Molecular & cellular oncology* **2014,** *1* (1), e29903-e29903.

85. Awasthi, P.; Foiani, M.; Kumar, A., ATM and ATR signaling at a glance. *Journal of Cell Science* **2015,** *128* (23), 4255-4262.

86. Ingenuity pathway analysis. Cell cycle: G2/m DNA damage checkpoint regulation. https://reports.ingenuity.com/rs/report/cpathway?id=ING%3Acig.

87. Bonda, D. J.; Lee, H.-G.; Camins, A.; Pallàs, M.; Casadesus, G.; Smith, M. A.; Zhu, X., The sirtuin pathway in ageing and Alzheimer disease: mechanistic and therapeutic considerations. *The Lancet. Neurology* **2011,** *10* (3), 275-279.

88. Di Franco, S.; Turdo, A.; Todaro, M.; Stassi, G., Role of Type I and II Interferons in Colorectal Cancer and Melanoma. *Frontiers in immunology* **2017,** *8*, 878-878.

89. Katlinskaya, Y. V.; Katlinski, K. V.; Yu, Q.; Ortiz, A.; Beiting, D. P.; Brice, A.; Davar, D.; Sanders, C.; Kirkwood, J. M.; Rui, H.; Xu, X.; Koumenis, C.; Diehl, J. A.; Fuchs, S. Y., Suppression of Type I Interferon Signaling Overcomes Oncogene-Induced Senescence and Mediates Melanoma Development and Progression. *Cell Reports* **2016,** *15* (1), 171-180.

90. Mammen, P. P.; Kanatous, S. B.; Yuhanna, I. S.; Shaul, P. W.; Garry, M. G.; Balaban, R. S.; Garry, D. J., Hypoxia-induced left ventricular dysfunction in myoglobin-deficient mice. *Am J Physiol Heart Circ Physiol* **2003,** *285* (5), H2132-41.

91. Grange, R. W.; Meeson, A.; Chin, E.; Lau, K. S.; Stull, J. T.; Shelton, J. M.; Williams, R. S.; Garry, D. J., Functional and molecular adaptations in skeletal muscle of myoglobin-mutant mice. *Am J Physiol Cell Physiol* **2001,** *281* (5), C1487-94.

92. Yamazaki, D.; Komazaki, S.; Nakanishi, H.; Mishima, A.; Nishi, M.; Yazawa, M.; Yamazaki, T.; Taguchi, R.; Takeshima, H., Essential role of the TRIC-B channel in Ca2+ handling of alveolar epithelial cells and in perinatal lung maturation. *Development* **2009,** *136* (14), 2355-61.

93. R, F.; S, Z.; M, B.; P, R.; S, V.; R, C.; H, K.; JE, G.; G, D. S.; S, G., Parkinson disease-associated DJ-1 is required for the expression of the glial cell line-derived neurotrophic factor receptor RET in human neuroblastoma cells. *J Biol Chem* **2010,** *285* (24), 18565-74. Epub 2010 Apr 15.

94. Flamini, M. I.; Gauna, G. V.; Sottile, M. L.; Nadin, B. S.; Sanchez, A. M.; Vargas-Roig, L. M., Retinoic acid reduces migration of human breast cancer cells: role of retinoic acid receptor beta. *Journal of cellular and molecular medicine* **2014,** *18* (6), 1113-1123.

95. Huang, M.; Qiu, Q.; Xiao, Y.; Zeng, S.; Zhan, M.; Shi, M.; Zou, Y.; Ye, Y.; Liang, L.; Yang, X.; Xu, H., BET Bromodomain Suppression Inhibits VEGF-induced Angiogenesis and Vascular Permeability by Blocking VEGFR2-mediated Activation of PAK1 and eNOS. *Scientific reports* **2016,** *6*, 23770-23770.

96. Tang, X.; Peng, R.; Phillips, J. E.; Deguzman, J.; Ren, Y.; Apparsundaram, S.; Luo, Q.; Bauer, C. M.; Fuentes, M. E.; DeMartino, J. A.; Tyagi, G.; Garrido, R.; Hogaboam, C. M.;

Denton, C. P.; Holmes, A. M.; Kitson, C.; Stevenson, C. S.; Budd, D. C., Assessment of Brd4 Inhibition in Idiopathic Pulmonary Fibrosis Lung Fibroblasts and in Vivo Models of Lung Fibrosis. *The American Journal of Pathology* **2013,** *183* (2), 470-479.

97. Wang, P.; Wang, F.; Wang, L.; Pan, J., Proprotein convertase subtilisin/kexin type 6 activates the extracellular signal-regulated kinase 1/2 and Wnt family member 3A pathways and promotes in vitro proliferation, migration and invasion of breast cancer MDA-MB-231 cells. *Oncol Lett* **2018,** *16* (1), 145-150.

98. Yang, J.; Bielenberg, D. R.; Rodig, S. J.; Doiron, R.; Clifton, M. C.; Kung, A. L.; Strong, R. K.; Zurakowski, D.; Moses, M. A., Lipocalin 2 promotes breast cancer progression. *Proc Natl Acad Sci U S A* **2009,** *106* (10), 3913-8.

99. Rodrigues-Ferreira, S.; Abdelkarim, M.; Dillenburg-Pilla, P.; Luissint, A.-C.; di-Tommaso, A.; Deshayes, F.; Pontes, C. L. S.; Molina, A.; Cagnard, N.; Letourneur, F.; Morel, M.; Reis, R. I.; Casarini, D. E.; Terris, B.; Couraud, P.-O.; Costa-Neto, C. M.; Di Benedetto, M.; Nahmias, C., Angiotensin II Facilitates Breast Cancer Cell Migration and Metastasis. *PLOS ONE* **2012,** *7* (4), e35667.

100. Dwyer, A. R.; Greenland, E. L.; Pixley, F. J., Promotion of Tumor Invasion by Tumor-Associated Macrophages: The Role of CSF-1-Activated Phosphatidylinositol 3 Kinase and Src Family Kinase Motility Signaling. *Cancers* **2017,** *9* (6), 68.

101. Prager, G. W.; Lackner, E.-M.; Krauth, M.-T.; Unseld, M.; Poettler, M.; Laffer, S.; Cerny-Reiterer, S.; Lamm, W.; Kornek, G. V.; Binder, B. R.; Zielinski, C. C.; Valent, P., Targeting of VEGF-dependent transendothelial migration of cancer cells by bevacizumab. *Molecular oncology* **2010,** *4* (2), 150-160.

102. Gómez-Contreras, P.; Ramiro-Díaz, J. M.; Sierra, A.; Stipp, C.; Domann, F. E.; Weigel, R. J.; Lal, G., Extracellular matrix 1 (ECM1) regulates the actin cytoskeletal architecture of aggressive breast cancer cells in part via S100A4 and Rho-family GTPases. *Clinical & experimental metastasis* **2017,** *34* (1), 37-49.

103. Marsigliante, S.; Vetrugno, C.; Muscella, A., CCL20 induces migration and proliferation on breast epithelial cells. *Journal of cellular physiology* **2013,** *228* (9), 1873-83.

104. Perisic, L.; Hedin, E.; Razuvaev, A.; Lengquist, M.; Osterholm, C.; Folkersen, L.; Gillgren, P.; Paulsson-Berne, G.; Ponten, F.; Odeberg, J.; Hedin, U., Profiling of atherosclerotic lesions by gene and tissue microarrays reveals PCSK6 as a novel protease in unstable carotid atherosclerosis. *Arterioscler Thromb Vasc Biol* **2013,** *33* (10), 2432-43.

105. Jiang, W.; Constante, M.; Santos, M. M., Anemia upregulates lipocalin 2 in the liver and serum. *Blood cells, molecules & diseases* **2008,** *41* (2), 169-174.

106. Xie, G.; Liu, Y.; Yao, Q.; Zheng, R.; Zhang, L.; Lin, J.; Guo, Z.; Du, S.; Ren, C.; Yuan, Q.; Yuan, Y., Hypoxia-induced angiotensin II by the lactate-chymase-dependent mechanism mediates radioresistance of hypoxic tumor cells. *Sci Rep* **2017,** *7*, 42396.

107. Chaturvedi, P.; Gilkes, D. M.; Takano, N.; Semenza, G. L., Hypoxia-inducible factor-dependent signaling between triple-negative breast cancer cells and mesenchymal stem cells promotes macrophage recruitment. *Proceedings of the National Academy of Sciences* **2014,** *111* (20), E2120-E2129.

108. Bosco, M. C.; Puppo, M.; Santangelo, C.; Anfosso, L.; Pfeffer, U.; Fardin, P.; Battaglia, F.; Varesio, L., Hypoxia modifies the transcriptome of primary human monocytes: modulation of novel immune-related genes and identification of CC-chemokine ligand 20 as a new hypoxia-inducible gene. *J Immunol* **2006,** *177* (3), 1941-55.

109. Rockland. p53 signaling pathway overview. https://rockland-inc.com/p53-pathway.aspx.

110. Koumenis, C.; Alarcon, R.; Hammond, E.; Sutphin, P.; Hoffman, W.; Murphy, M.; Derr, J.; Taya, Y.; Lowe, S. W.; Kastan, M.; Giaccia, A., Regulation of p53 by hypoxia: dissociation of transcriptional repression and apoptosis from p53-dependent transactivation. *Molecular and cellular biology* **2001,** *21* (4), 1297-1310.

111. Sethy, N. K.; Singh, M.; Kumar, R.; Ilavazhagan, G.; Bhargava, K., Upregulation of transcription factor NRF2-mediated oxidative stress response pathway in rat brain under short-term chronic hypobaric hypoxia. *Funct Integr Genomics* **2011,** *11* (1), 119-37.

112. Kanasaki, K.; Palmsten, K.; Sugimoto, H.; Ahmad, S.; Hamano, Y.; Xie, L.; Parry, S.; Augustin, H. G.; Gattone, V. H.; Folkman, J.; Strauss, J. F.; Kalluri, R., Deficiency in catechol-O-methyltransferase and 2-methoxyoestradiol is associated with pre-eclampsia. *Nature* **2008,** *453* (7198), 1117-21.

113. Hu, W.; Lu, C.; Dong, H. H.; Huang, J.; Shen, D. Y.; Stone, R. L.; Nick, A. M.; Shahzad, M. M.; Mora, E.; Jennings, N. B.; Lee, S. J.; Roh, J. W.; Matsuo, K.; Nishimura, M.; Goodman, B. W.; Jaffe, R. B.; Langley, R. R.; Deavers, M. T.; Lopez-Berestein, G.; Coleman, R. L.; Sood, A. K., Biological roles of the Delta family Notch ligand Dll4 in tumor and endothelial cells in ovarian cancer. *Cancer Res* **2011,** *71* (18), 6030-9.

114. Ma, Y.; Iyer, R. P.; de Castro Brás, L. E.; Toba, H.; Yabluchanskiy, A.; Deleon-Pennell, Kristine Y.; Hall, M. E.; Lange, R. A.; Lindsey, M. L., Chapter 4 - Cross Talk Between Inflammation and Extracellular Matrix Following Myocardial Infarction. In *Inflammation in Heart Failure*, Blankesteijn, W. M.; Altara, R., Eds. Academic Press: Boston, 2015; pp 67-79.

115. Kerbel, R. S., Tumor angiogenesis. *The New England journal of medicine* **2008,** *358* (19), 2039-2049.

116. Payne, S. L.; Fogelgren, B.; Hess, A. R.; Seftor, E. A.; Wiley, E. L.; Fong, S. F.; Csiszar, K.; Hendrix, M. J.; Kirschmann, D. A., Lysyl oxidase regulates breast cancer cell migration and adhesion through a hydrogen peroxide-mediated mechanism. *Cancer research* **2005,** *65* (24), 11429-36.

117. Zhou, Z. N.; Sharma, V. P.; Beaty, B. T.; Roh-Johnson, M.; Peterson, E. A.; Van Rooijen, N.; Kenny, P. A.; Wiley, H. S.; Condeelis, J. S.; Segall, J. E., Autocrine HBEGF expression promotes breast cancer intravasation, metastasis and macrophage-independent invasion in vivo. *Oncogene* **2014,** *33* (29), 3784-3793.

118. Guo, D.; Huang, J.; Gong, J., Bone morphogenetic protein 4 (BMP4) is required for migration and invasion of breast cancer. *Molecular and cellular biochemistry* **2012,** *363* (1-2), 179-90.

119. Kontomanolis, E.; Panteliadou, M.; Giatromanolaki, A.; Pouliliou, S.; Efremidou, E.; Limberis, V.; Galazios, G.; Sivridis, E.; Koukourakis, M. I., Delta-like ligand 4 (DLL4) in the plasma and neoplastic tissues from breast cancer patients: correlation with metastasis. *Med Oncol* **2014,** *31* (5), 945.

120. Murai, R.; Tanaka, M.; Takahashi, Y.; Kuribayashi, K.; Kobayashi, D.; Watanabe, N., Stanniocalcin-1 promotes metastasis in a human breast cancer cell line through activation of PI3K. *Clin Exp Metastasis* **2014,** *31* (7), 787-94.

121. Kulkarni, A. H.; Chatterjee, A.; Kondaiah, P.; Gundiah, N., TGF-beta induces changes in breast cancer cell deformability. *Phys Biol* **2018,** *15* (6), 065005.

122. Topcu, T. O.; Kavgaci, H.; Gunaldi, M.; Kocoglu, H.; Akyol, M.; Mentese, A.; Yaman, S. O.; Orem, A.; Ozdemir, F.; Aydin, F., The clinical importance of serum galectin-3 levels in

breast cancer patients with and without metastasis. *J Cancer Res Ther* **2018,** *14* (Supplement), S583-s586.

123. Salomon, D. S.; Normanno, N.; Ciardiello, F.; Brandt, R.; Shoyab, M.; Todaro, G. J., The role of amphiregulin in breast cancer. *Breast Cancer Res Treat* **1995,** *33* (2), 103-14.

124. Xie, Q.; Xie, J.; Tian, T.; Ma, Q.; Zhang, Q.; Zhu, B.; Cai, X., Hypoxia triggers angiogenesis by increasing expression of LOX genes in 3-D culture of ASCs and ECs. *Exp Cell Res* **2017,** *352* (1), 157-163.

125. Sakai, M.; Tsukada, T.; Harris, R. C., Oxidant stress activates AP-1 and heparin-binding epidermal growth factor-like growth factor transcription in renal epithelial cells. *Exp Nephrol* **2001,** *9* (1), 28-39.

126. Wu, D.-C.; Paulson, R. F., Hypoxia regulates BMP4 expression in the murine spleen during the recovery from acute anemia. *PloS one* **2010,** *5* (6), e11303-e11303.

127. Irshad, K.; Mohapatra, S. K.; Srivastava, C.; Garg, H.; Mishra, S.; Dikshit, B.; Sarkar, C.; Gupta, D.; Chandra, P. S.; Chattopadhyay, P.; Sinha, S.; Chosdol, K., A combined gene signature of hypoxia and notch pathway in human glioblastoma and its prognostic relevance. *PloS one* **2015,** *10* (3), e0118201-e0118201.

128. Yeung, H. Y.; Lai, K. P.; Chan, H. Y.; Mak, N. K.; Wagner, G. F.; Wong, C. K., Hypoxia-inducible factor-1-mediated activation of stanniocalcin-1 in human cancer cells. *Endocrinology* **2005,** *146* (11), 4951-60.

129. Mingyuan, X.; Qianqian, P.; Shengquan, X.; Chenyi, Y.; Rui, L.; Yichen, S.; Jinghong, X., Hypoxia-inducible factor-1α activates transforming growth factor-β1/Smad signaling and increases collagen deposition in dermal fibroblasts. *Oncotarget* **2017,** *9* (3), 3188-3197.

130. Howe, A. K., Regulation of actin-based cell migration by cAMP/PKA. *Biochim Biophys Acta* **2004,** *1692* (2-3), 159-74.

131. Haga, R. B.; Ridley, A. J., Rho GTPases: Regulation and roles in cancer cell biology. *Small GTPases* **2016,** *7* (4), 207-221.